# PCSK9 Induces CD36 Degradation and Affects Long-Chain Fatty Acid Uptake and Triglyceride Metabolism in Adipocytes and in Mouse Liver

Annie Demers, Samaneh Samami, Benjamin Lauzier, Christine Des Rosiers, Emilienne Tudor Ngo Sock, Huy Ong, Gaetan Mayer

# PCSK9 Induces CD36 Degradation and Affects Long-Chain Fatty Acid Uptake and Triglyceride Metabolism in Adipocytes and in Mouse Liver

Annie Demers, Samaneh Samami, Benjamin Lauzier, Christine Des Rosiers, Emilienne Tudor Ngo Sock, Huy Ong, Gaetan Mayer

***Objective***—Proprotein convertase subtilisin/kexin type 9 (PCSK9) promotes the degradation of the low-density lipoprotein receptor thereby elevating plasma low-density lipoprotein cholesterol levels and the risk of coronary heart disease. Thus, the use of PCSK9 inhibitors holds great promise to prevent heart disease. Previous work found that PCSK9 is involved in triglyceride metabolism, independently of its action on low-density lipoprotein receptor, and that other yet unidentified receptors could mediate this effect. Therefore, we assessed whether PCSK9 enhances the degradation of CD36, a major receptor involved in transport of long-chain fatty acids and triglyceride storage.

***Approach and Results***—Overexpressed or recombinant PCSK9 induced CD36 degradation in cell lines and primary adipocytes and reduced the uptake of the palmitate analog Bodipy FL $C_{16}$ and oxidized low-density lipoprotein in 3T3-L1 adipocytes and hepatic HepG2 cells, respectively. Surface plasmon resonance, coimmunoprecipitation, confocal immunofluorescence microscopy, and protein degradation pathway inhibitors revealed that PCSK9 directly interacts with CD36 and targets the receptor to lysosomes through a mechanism involving the proteasome. Importantly, the level of CD36 protein was increased by >3-fold upon small interfering RNA knockdown of endogenous PCSK9 in hepatic cells and similarly increased in the liver and visceral adipose tissue of *Pcsk9*$^{-/-}$ mice. In *Pcsk9*$^{-/-}$ mice, increased hepatic CD36 was correlated with an amplified uptake of fatty acid and accumulation of triglycerides and lipid droplets.

***Conclusions***—Our results demonstrate an important role of PCSK9 in modulating the function of CD36 and triglyceride metabolism. PCSK9-mediated CD36 degradation may serve to limit fatty acid uptake and triglyceride accumulation in tissues, such as the liver. **(*Arterioscler Thromb Vasc Biol*. 2015;35:2517-2525. DOI: 10.1161/ATVBAHA.115.306032.)**

**Key Words:** antigens, CD36 ■ mice, knockout ■ Pcsk9 protein, mouse ■ receptors, LDL ■ triglyceride



Maintenance of optimal blood lipid levels is central to vascular health. Dysregulation of circulating lipid homeostasis, such as elevated levels of low-density lipoprotein cholesterol (LDLc) and triglycerides, is associated with premature atherosclerosis and coronary heart disease.[1] Naturally occurring genetic variations at the proprotein convertase subtilisin/kexin type 9 (*PCSK9*) locus are major determinant of plasma LDLc levels in humans.[2] PCSK9 promotes the degradation of the hepatic LDL receptor (LDLR), the primary pathway of LDLc uptake from the circulation, thereby causing LDLc levels to rise.[3] Gain-of-function mutations in PCSK9 can cause autosomal dominant hypercholesterolemia and premature death resulting from coronary atherosclerosis.[4,5] Remarkably, PCSK9 loss-of-function mutations lower circulating LDLc and are associated with strikingly reduced incidence of coronary heart disease.[6] As a result, inhibitors of PCSK9 are being developed and tested in clinical trials with the ultimate goal of lowering risk of heart diseases.[7]

PCSK9 is a secretory serine protease mainly expressed by the liver, intestine, and kidney.[8,9] Unlike other proprotein convertases that lose their prosegment and are activated in the late secretory pathway,[10] PCSK9 is secreted in complex with its prosegment trapped in the catalytic pocket.[11] Hence, PCSK9 induces LDLR degradation independently of its catalytic activity.[12] PCSK9 interacts with the LDLR epidermal growth factor–like repeat A (EGFA) domain at the cell surface[13] and is internalized in endosomes, where its affinity for the receptor increases by several fold,[11] thereby impeding LDLR recycling to the cell surface and promoting its degradation by lysosomal hydrolases.[3,13] A previous study demonstrated that PCSK9

Received on: June 9, 2015; final version accepted on: October 12, 2015.

From the Laboratory of Molecular Cell Biology (A.D., S.S., E.T.N.S., G.M.) and Laboratory of Metabolomic (C.D.R.), Montreal Heart Institute, Montréal, Québec, Canada; Université de Nantes, L'institut du thorax, Inserm UMR 1087 / CNRS UMR 6291, Nantes, France (B.L.); and Faculty of Pharmacy (H.O.), Université de Montréal, Department of Pharmacology, Faculty of Medicine (S.S., E.T.N.S., G.M.), Department of Nutrition, Faculty of Medicine (C.D.R.), and Department of Medicine (G.M.), Faculty of Medicine, Université de Montréal, Montréal, Québec, Canada.

**The online-only Data Supplement is available with this article at http://atvb.ahajournals.org/lookup/suppl/doi:10.1161/ATVBAHA.115.306032/-/DC1.**

Correspondence to Gaetan Mayer, PhD, Laboratory of Molecular Cell Biology, Montreal Heart Institute Research Center, 5000 Bélanger St, Room S-5350, Montréal, Québec H1T1C8, Canada. E-mail gaetan.mayer@icm-mhi.org

| Nonstandard Abbreviations and Acronyms | |
|---|---|
| **CD36** | cluster of differentiation 36 |
| **LDL** | low-density lipoprotein |
| **LDLc** | LDL cholesterol |
| **LDLR** | LDL receptor |
| **PCSK9** | proprotein convertase subtilisin/kexin type 9 |
| **SRB3** | scavenger receptor class B type 3 |
| **WT** | wild type |

enhances the degradation of other receptors, such as the very low-density lipoprotein receptor and apolipoprotein E receptor 2, the closest structural members to LDLR, emphasizing its major role in cholesterol and lipid homeostasis.[14] Furthermore, PCSK9 induces the degradation of CD81, a receptor for hepatitis C virus,[15] the epithelial sodium channel (ENaC),[16] and β-secretase 1 (BACE1).[17] Hence, PCSK9 targets multiple proteins and receptors, of which some are not related to the LDLR family, suggesting that the convertase has other metabolic roles. Indeed, plasma PCSK9 levels correlate with multiple metabolic markers, such as fasting levels of glucose, insulin, triglycerides, and hepatic triglycerides content, indicating that it could target other receptors that remain to be uncovered.[18,19]

Cluster of differentiation 36 (CD36; scavenger receptor class B type 3 [SRB3] or fatty acid translocase) is a member of the scavenger receptor class B family that includes SRB1, the high-density lipoprotein receptor mediating cholesteryl ester uptake, and SRB2, a lysosomal integral membrane protein (LIMP2).[20] CD36 has a hairpin-like structure with a large and extensively N-glycosylated extracellular loop, the C and N termini spanning the membrane and 2 cytosolic tails. It is a multiligand cell surface receptor expressed in several cells and tissues, such as macrophages, heart, adipose tissue, and liver.[20] CD36 is a major receptor for oxidized LDL in macrophages and plays a critical role in the formation of lipid-laden foam cells and atherosclerosis. CD36 also contributes to muscle lipid utilization, adipose energy storage, and fat absorption in tissues with important lipid fluxes by binding long-chain fatty acids and facilitating their transport into cells.[20] Recently, it has become apparent that CD36 also plays an important role in the liver by participating in the uptake of fatty acids and in triglyceride storage and secretion. Because of its function in lipid metabolism, CD36 has been linked to insulin resistance, obesity, and type 2 diabetes mellitus.[21]

PCSK9 and CD36 are both involved in the complex regulation of lipid and triglyceride metabolism, and therefore, we undertook to study their functional relationship. Herein, we show that PCSK9 induces the degradation of CD36 and regulates its function in mouse and human cell lines and in mice. Through direct protein–protein interaction, PCSK9 provokes CD36 degradation by a mechanism that depends on both lysosomal and proteasomal activity, which affects the uptake of CD36 ligands in adipocytes and hepatic cells. In *Pcsk9*$^{-/-}$ mice, CD36 protein levels were significantly increased in visceral adipose tissue and in the liver. Correspondingly, hepatic triglyceride content and uptake of long-chain fatty acids were found to be increased in the absence of PCSK9. Together, our data demonstrate that PCSK9 has an additional role in lipid homeostasis beyond its effect on LDLc through the regulation of CD36 levels and function.

## Materials and Methods

Materials and Methods are available in the online-only Data Supplement.

## Results

### PCSK9 Induces the Degradation of CD36 Through a Proteasome-Sensitive Mechanism in a Post-Endoplasmic Reticulum, Acidic Compartment

To determine whether PCSK9 regulates the protein level of CD36 by enhancing its degradation, we first used HEK293 cells, which can be transfected with high efficiency. Cotransfection of hemagglutinin (HA)-tagged CD36 (CD36-HA) and increasing amount of PCSK9-V5 cDNA demonstrated that, similar to LDLR, PCSK9 dose dependently decreases CD36 protein levels by up to ≈70% (Figure 1A and 1B). Although CD36 protein levels were decreased only on its cotransfection with PCSK9 (Figure 1C), the level of its paralog LIMP2 was not modified by PCSK9, as previously reported for SRB1,[22] or by any of the other proprotein convertases tested (proprotein convertase 5A [PC5A], subtilisin kexin isozyme-1 [SKI-1], or Furin; Figure 1D) attesting for the specificity of the PCSK9-induced CD36 degradation. The degradation of CD36 was also tested in the human hepatic cell line HepG2, which is commonly used to study PCSK9 function,[12] stably expressing CD36-HA (Figure 1E). Transfection of these cells with PCSK9-V5 cDNA demonstrated a dose-dependent reduction of CD36 protein level (Figure 1F, first 4 lanes), which correlated with decreased internalization of CD36 ligand DiI-oxLDL (Figure 1G). Of note, Western blotting of CD36 yielded 2 bands in HepG2 cells, which are both reduced in the presence of PCSK9 (Figure 1F), likely reflecting differential glycosylation compared with HEK293 cells (Figure 1A and 1C). The PCSK9-induced degradation of CD36 was inhibited by the lysosomal function inhibitor ammonium chloride ($NH_4Cl$) and the vesicle trafficking inhibitor brefeldin A (Figure 1F), suggesting that transport out of the endoplasmic reticulum and an acidic compartment are required, as previously shown for LDLR degradation.[3] Interestingly, the effect of PCSK9 was also reversed by MG132 (Figure 1F), suggesting the involvement of the proteasome, which does not participate in the PCSK9-induced degradation of LDLR.[3] Moreover, the use of a panel of proteasome inhibitors, ALLN (N-acetyl-L-leucyl-L-leucyl-L-norleucinal), lactacystin, proteasome inhibitor-1, or MG132, resulted in the inhibition of the PCSK9-induced CD36 degradation but not of LDLR degradation (Figure IA in the online-only Data Supplement). These results indicate that PCSK9 induces the degradation of CD36 by a mechanism that requires both proteasome and endosomes/lysosomes.

We next evaluated the regulation of CD36 protein expression by endogenous PCSK9 in HepG2-CD36 cells. Transfection of a specific small interfering RNA against human PCSK9 in HepG2 cells resulted in a knockdown of >85% and caused a robust increased of CD36 protein level, as well as that of LDLR (Figure 1H). Then, to determine whether

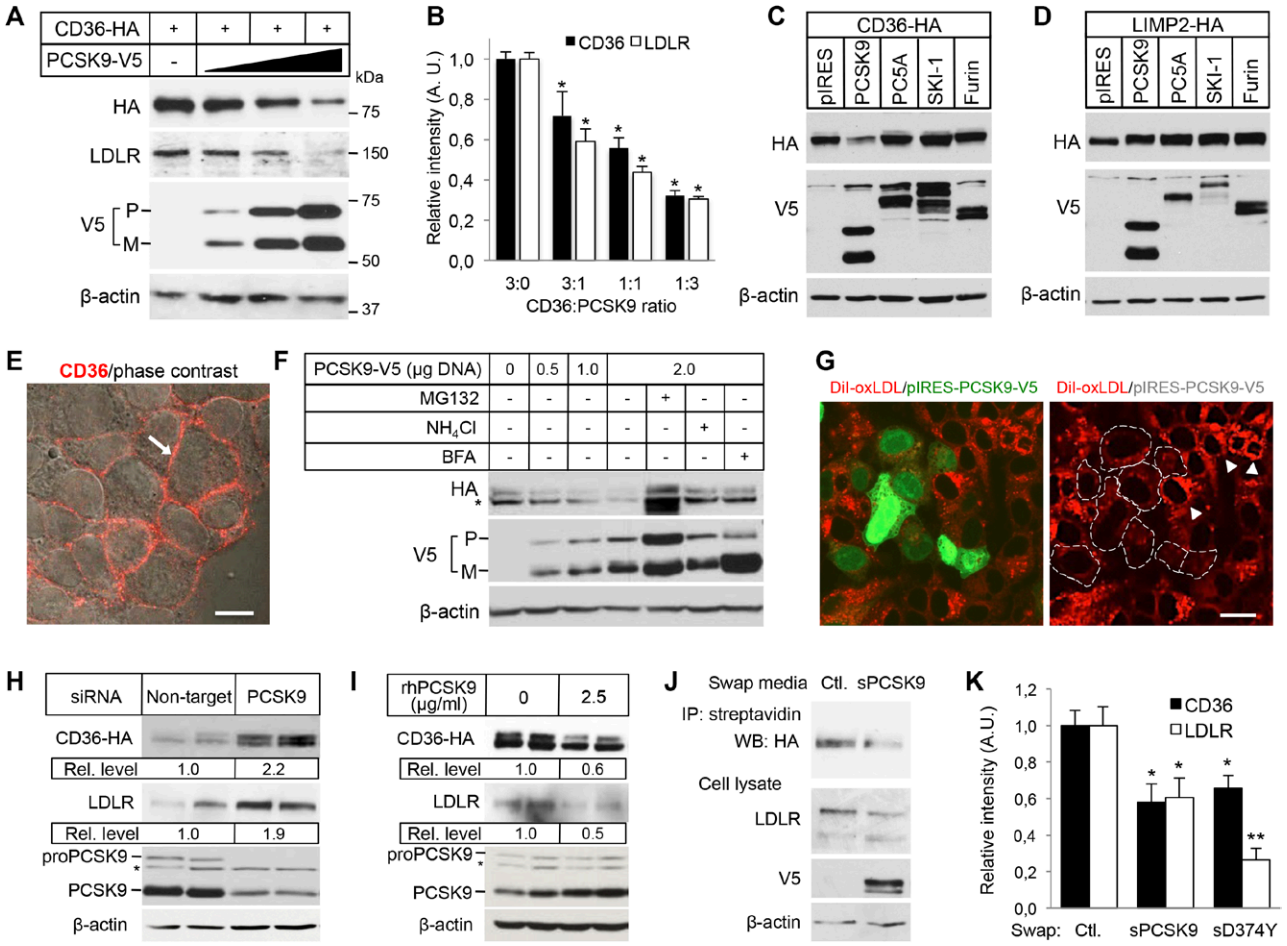


**Figure 1.** Proprotein convertase subtilisin/kexin type 9 (PCSK9) induces cluster of differentiation 36 (CD36) degradation. **A**, HEK293 cells transfected with CD36-HA cDNA (0.15 μg) and either with an empty pIRES-V5 vector (–) or with increasing amounts of PCSK9-V5 cDNA (lane 2, 0.05 μg; lane 3, 0.15 μg; and lane 4, 0.45 μg). Cell lysates were subjected to Western blotting (WB) with the anti-HA, anti-human (h)LDLR, anti-V5-horseradish peroxidase (HRP), and anti-β-actin antibodies. M indicates mature PCSK9; and P, pro-PCSK9. **B**, Densitometry calculations for WB data as shown in (**A**). The relative density of the bands was normalized to β-actin (n=10 per condition). **P*<0.01 vs 3:0 ratio. **C** and **D**, WB analysis of CD36 and lysosomal integral membrane protein (LIMP2; anti-HA antibody) and proprotein convertases (anti-V5-HRP antibody) in lysates of HEK293 cells transfected with CD36-HA (**C**) or LIMP2-HA (**D**) and either with an empty pIRES-V5 vector (pIRES) or with V5-tagged PCSK9, PC5A, SKI-1, or Furin. β-actin was used as a control for loading. **E**, Immunolabeling of cell surface CD36 (arrow) in unpermeabilized stable HepG2-CD36-HA cells. Bar, 20 μm. **F**, Stable HepG2-CD36-HA cells transiently transfected with increasing amounts of PCSK9-V5 plasmid in the presence or absence of 1 μmol/L MG132, 10 mmol/L ammonium chloride (NH4Cl), or 5 μg/mL brefeldin A (BFA). CD36 (anti-HA), PCSK9 (anti-V5-HRP), and actin (anti-β-actin) were analyzed by WB. The asterisk denotes an additional band likely reflecting differential CD36 glycosylation in HepG2 cells compared with HEK293 cells (**A** and **C**). **G**, Stable HepG2-CD36-HA cells transiently transfected with PCSK9-V5 (transfected cells express EGFP [green nuclei]) were incubated with DiI-oxLDL (red) for 1 h at 37°C and fixed for fluorescence analysis. The dashed lines (**right**) outline PCSK9-expressing cells with low content of DiI-oxLDL compared with nontransfected cells (arrowheads). Bar, 20 μm. **H** and **I**, WB for CD36 (anti-HA), LDLR (anti-hLDLR), PCSK9 (anti-hPCSK9, which detects endogenous PCSK9 and rhPCSK9), and β-actin (anti-β-actin) in lysates of stable HepG2-CD36-HA cells transfected with an small interfering RNA (siRNA) targeting human PCSK9 or a control nontarget siRNA (**H**), or incubated with or without 2.5 μg/mL rhPCSK9 for 16 h (**I**). The asterisk indicates a nonspecific band. **J**, Stable HepG2-CD36-HA cells were incubated with conditioned media of HEK293 cells overexpressing pIRES-V5 (control) or V5-tagged PCSK9 (sPCSK9) for 16 h. Cell surface proteins were biotinylated, and cell lysates were either affinity precipitated with streptavidin agarose and analyzed by WB for CD36 (anti-HA) or analyzed by WB for LDLR (anti-hLDLR), PCSK9 (anti-V5-HRP), and β-actin (anti-β-actin). **K**, Quantification of band intensity for CD36 and LDLR from HepG2-CD36-HA cells treated with control medium (pIRES-V5, Ctl.) or V5-tagged PCSK9 (sPCSK9) or D374Y mutant, as described in (**J**). WB signals were normalized to β-actin. n=5 independent experiments for each condition. **P*<0.01; ***P*<0.001 vs control. LDLR indicates low-density lipoprotein receptor.

PCSK9 can induce CD36 degradation through an extracellular pathway,[7] HepG2-CD36 cells were incubated with physiological levels of recombinant human PCSK9[18] (2.5 μg/mL rhPCSK9; Figure IB in the online-only Data Supplement). Western blotting results demonstrated that PCSK9 was capable of inducing the degradation of both CD36 and LDLR via an extracellular pathway (Figure 1I). In addition, secreted PCSK9 from conditioned media of HEK293 cells expressing PCSK9-V5 (2 μg/mL sPCSK9; Figure IB in the online-only Data Supplement) reduced the levels of cell surface CD36 in HepG2-CD36 cells (Figure 1J). Interestingly, the PCSK9-D374Y mutant did not result in a gain-of-function over CD36 as it does for LDLR[5,7] (Figure 1K), suggesting that PCSK9 has different binding requirement for both receptors.

## PCSK9 Directly Interacts With CD36

We then sought to evaluate direct protein–protein interaction of PCSK9 and CD36. Using surface plasmon resonance, we found that purified rhPCSK9 bound to the immobilized extracellular domain of CD36 (hCD36ED) in a concentration-dependent manner with a dissociation constant ($K_d$) of 1.2 µmol/L at pH 7.4 (Figure 2A), which is similar to the reported Kd of CD36 ligands[23] and similar to the Kd of PCSK9 binding to the LDLR EGFA domain (≈0.63–1 µmol/L at neutral pH).[24,25] In addition, coimmunoprecipitation and confocal microscopy experiments showed that PCSK9 was specifically pulled down with CD36 and colocalized with the receptor in lysosomes in HEK293 cells (Figure 2B and 2C; Figure II in the online-only Data Supplement). This prompted us to test whether PCSK9 binding to LDLR was required for CD36 degradation. The PCSK9-F379A mutant, a PCSK9 loss-of-function mutation that does not interact with LDLR,[26] was found to coimmunoprecipitate with CD36 and induced its degradation, with even more potency than wild-type (WT) PCSK9, but not that of LDLR (Figure IIIA and IIIB in the online-only Data Supplement). In addition, knockdown of LDLR (>90%) did not impeded PCSK9-induced CD36 degradation, suggesting that the PCSK9–LDLR interaction is not a requisite for CD36 degradation (Figure IIIC in the online-only Data Supplement). However, a PCSK9 neutralizing antibody that inhibits LDLR degradation also interfered with the extracellular pathway of CD36 degradation (Figure IIID in the online-only Data Supplement), suggesting that the catalytic domain of PCSK9, which is targeted by the neutralizing antibody, or a nearby region is involved in regulating CD36 protein levels.

## PCSK9 Reduces Long-Chain Fatty Acid Uptake in Adipocytes and Regulates CD36 Protein Level in Visceral Adipose Tissue of *Pcsk9*$^{-/-}$ Mice

We next assessed the PCSK9-mediated regulation of endogenous CD36 in cell lines and tissues. Both PCSK9 and CD36 are well expressed in the small intestine.[8,27] CD36 is highly expressed on the luminal surface of enterocytes in fasted mice and is degraded through a ubiquitin-dependent pathway in response to feeding.[27] Therefore, we explored the effect of nutritional status on CD36 expression in the intestine of WT and *Pcsk9*$^{-/-}$ mice. Immunofluorescence of CD36 in the jejunum showed a weak staining in both genotypes under fed conditions and was remarkably increased at the apical surface of enterocytes under fasting conditions but without overt differences in intensity between WT and *Pcsk9*$^{-/-}$ mice (Figure IVA in the online-only Data Supplement). Similarly, CD36 levels were not significantly modified in the heart of *Pcsk9*$^{-/-}$ mice, whereas LDLR levels were slightly increased (Figure IVB in the online-only Data Supplement). Also, incubation of HL-1 cardiac muscle cells, with or without insulin stimulation,[28] and PMA (phorbol 12-myristate 13-acetate)-induced THP-1 macrophages with sPCSK9 revealed no modification of CD36 protein level, whereas that of LDLR was significantly decreased in HL-1 cells (LDLR was barely detectable in THP-1 cells; Figure IVC and IVD in the online-only Data Supplement). However, incubation of 3T3-L1 adipocytes and mouse primary adipocytes with sPCSK9 demonstrated a significant reduction of endogenous CD36 and LDLR (Figure 3A; Figure VA and VB in the online-only Data Supplement). Moreover, as shown for HepG2 (Figure 1F) and HEK293 cells (Figure I in the online-only Data Supplement), incubation of 3T3-L1

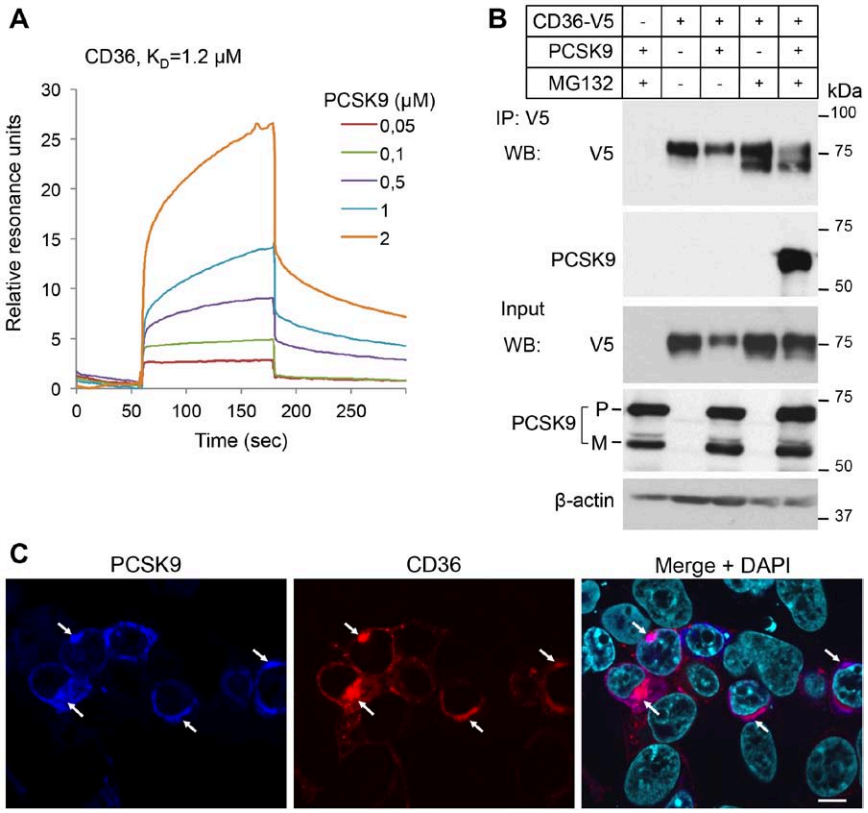


**Figure 2.** Proprotein convertase subtilisin/kexin type 9 (PCSK9) interacts and colocalizes with cluster of differentiation 36 (CD36). **A**, Purified recombinant PCSK9 (0.05–2 µmol/L) bound to the immobilized extracellular domain of CD36 with a $K_d$ of 1.2 µmol/L at pH 7.4, as determined using surface plasmon resonance. **B**, Western blotting (WB) showing coimmunoprecipitation of CD36 with PCSK9 from HEK293 cells expressing an empty pIRES-V5 vector (–) or CD36-V5 and untagged PCSK9 in the presence or absence of 1 µmol/L MG132. Immunoprecipitated proteins (IP: V5) were detected by WB using the anti-V5-HRP and anti-hPCSK9 antibodies. Immunoblots of CD36-V5, PCSK9, and β-actin before IP (input) are shown. **C**, Immunofluorescence of HEK293 cells cotransfected with PCSK9-V5 and CD36-HA in the presence of 1 µmol/L MG132. Immunolabeling was performed under permeabilizing condition with the anti-V5 (blue) and anti-HA (red) antibodies. Colocalization (arrows) of PCSK9 with CD36 is exemplified by the purple color in the merge image. Nuclei were stained using DAPI (cyan). Bar, 10 µm. M indicates mature PCSK9; and P, pro-PCSK9.

adipocytes with inhibitors of the proteasome (MG132 or lactacystin) or 3 different lysosome inhibitors ($NH_4Cl$, E64D (cysteine proteases inhibitor), or bafilomycin A1 (vacuolar type H+-ATPase [V-ATPase inhibitor]) inhibited the PCSK9-induced degradation of CD36 (Figure 3A; Figure VC in the online-only Data Supplement). MG132 had a slight effect on LDLR levels in adipocytes likely because of nonspecific inhibition of lysosomal enzymes.[29]

To determine whether PCSK9 reduces cell surface CD36 and affects its function, 3T3-L1 adipocytes were incubated for 16 hours with sPCSK9 and then with Bodipy FL $C_{16}$ (Figure 3B). Compared with control medium, PCSK9-treated adipocytes showed a strong reduction of cell surface CD36 coinciding with significantly lower amount of internalized palmitate analog (Figure 3B). In addition, coimmunoprecipitation and confocal microscopy experiments from adipocytes incubated with 2 μg/mL purified rhPCSK9 revealed that endogenous CD36 interacts and colocalizes with PCSK9 at the cell surface and in vesicular endosome/lysosome-like compartments (Figure 3C and 3D; Figure VD in the

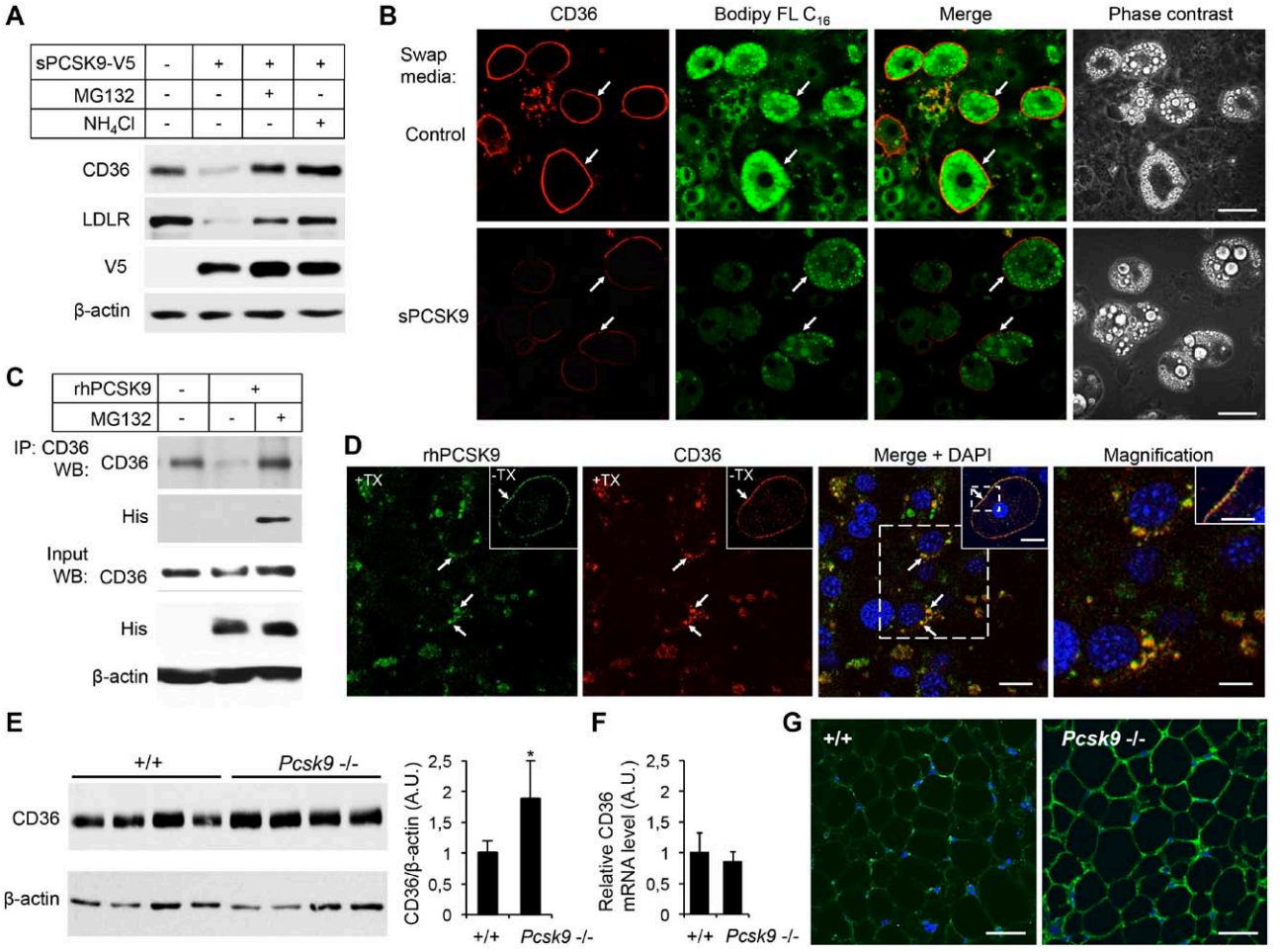


**Figure 3.** Proprotein convertase subtilisin/kexin type 9 (PCSK9) regulates endogenous cluster of differentiation 36 (CD36) in 3T3-L1 adipocytes and in mouse adipose tissue. **A**, Western blotting (WB) of CD36 (anti-mCD36), low-density lipoprotein receptor (LDLR; anti-mLDLR), PCSK9 (anti-V5-HRP), and actin (anti-β-actin) in differentiated 3T3-L1 adipocytes incubated for 16 h with conditioned media obtained from HEK293 cells transfected with an empty pIRES-V5 vector (–) or V5-tagged PCSK9 (secreted PCSK9, sPCSK9) in the absence or presence of 2.5 μmol/L MG132 or 10 mmol/L $NH_4Cl$. **B**, PCSK9-mediated degradation of CD36 reduces internalization of fatty acids. 3T3-L1 adipocytes were incubated for 16 h with control medium or with sPCSK9 as described in (**A**) and then incubated with Bodipy FL $C_{16}$ for 30 min. Cell surface immunofluorescence of endogenous CD36 in nonpermeabilized cells (arrows) was performed using anti-mCD36. Confocal images of CD36 (red) and Bodipy FL $C_{16}$ (green) were acquired at identical laser output, gain, and offset. Bar, 40 μm. **C**, Coimmunoprecipitation of endogenous CD36 with PCSK9 in 3T3-L1 adipocytes incubated for 16 h with DMEM (–) or with 2 μg/mL rhPCSK9 with or without 2.5 μmol/L MG132. Immunoprecipitation (IP) was performed using the anti-mCD36 antibody (IP: CD36). Immunoprecipitated proteins were analyzed by WB using anti-mCD36 and anti-His (to detect rhPCSK9) antibodies. Levels of CD36, rhPCSK9, and β-actin before IP (input) are shown. **D**, Confocal microscopy of 3T3-L1 adipocytes incubated with 2 μg/mL rhPCSK9 in the presence of 1 μmol/L MG132 for 16 h. Permeabilized cells (+Triton-X, TX) were immunolabeled with anti-hPCSK9 (green) and anti-mCD36 (red) antibodies. Arrows show colocalization of PCSK9 and CD36 in large vesicles in the perinuclear region. Bar, 20 μm. Insets show cell surface labeling and colocalization (arrow) of PCSK9 and CD36 in unpermeabilized (–TX) adipocytes. Bar, 20 μm. Magnified images of area within dashed square are shown (**right** and inset). Magnification: bars, 10 μm. **E**, WB of CD36 in perigonadal fat of 12-week-old C57BL/6 (+/+) and *Pcsk9*$^{-/-}$ mice. Quantification of the bands (**right**) was normalized to β-actin (n=4 mice/genotype). *$P$<0.05 vs +/+. **F**, Perigonadal fat CD36 mRNA levels as determined by quantitative polymerase chain reaction (n=5 mice/genotype). **G**, Representative immunofluorescence images of CD36 in perigonadal adipose tissue of 12-week-old C57BL/6 (+/+) and *Pcsk9*$^{-/-}$ mice. Bar, 50 μm. These data are representative of ≈3 independent experiments.

online-only Data Supplement). Importantly, CD36 protein levels, but not its mRNA expression, were found significantly increased by ≈80% in perigonadal fat pads of *Pcsk9*$^{-/-}$ mice when compared with control C57BL/6 (+/+) mice (Figure 3E and 3F). In support of these results, confocal immunofluorescence microscopy of CD36 in mouse adipose tissue showed a strong increase of the immunolabeling at the surface of adipocytes in *Pcsk9*$^{-/-}$ mice (Figure 3G). Taken together, these results demonstrate that PCSK9 interacts with and decreases endogenous cell surface CD36 thereby reducing internalization of fatty acids in adipocytes and also suggest that circulating PCSK9 modifies CD36 protein levels and function in visceral adipose tissue.

### CD36 Protein Levels, Long-Chain Fatty Acid Uptake, and Triglyceride Content Are Increased in the Liver of *Pcsk9*$^{-/-}$ Mice

PCSK9 is predominantly expressed in the liver and preferentially reduces LDLR protein levels in hepatocytes.[30] Thus, we tested whether hepatic CD36 was regulated in *Pcsk9*$^{-/-}$ mice. Our Western blotting results demonstrated that, compared with control +/+ mice and similar to LDLR, CD36 protein levels were strongly increased (≈3-fold, $P<0.001$) in membrane fractions of *Pcsk9*$^{-/-}$ liver, whereas SRB1 and pan-cadherin (herein used as membrane marker) levels were not modified (Figure 4A and 4B). Immunohistochemical analysis showed that CD36 was markedly increased at the basolateral plasma membrane of *Pcsk9*$^{-/-}$ hepatocytes, where it was colocalized with LDLR, a well-known basolateral membrane marker[31] (Figure 4C). Importantly, quantitative polymerase chain reaction analyses showed no variation in liver CD36 and LDLR mRNA levels between +/+ and *Pcsk9*$^{-/-}$ mice, indicating a post-translational regulation of the receptors by PCSK9 (Figure 4D).[3]

Accordingly, injection of rhPCSK9 to WT C57BL/6 mice, which reduces hepatic LDLR by ≈90% within 60 minutes (Figure VI in the online-only Data Supplement),[30] reduced hepatic CD36 levels by 57% after 60 minutes and by 66% after 120 minutes, demonstrating that circulating PCSK9 can induce the degradation of CD36 (Figure VI in the online-only Data Supplement). CD36 protein levels are directly related to fatty acid uptake and triglyceride storage in the liver.[21] Thus, we next compared hepatic lipid content and uptake in the absence or presence of PCSK9. Remarkably, neutral lipid staining of liver cryosections and quantification of triglycerides in liver extracts of *Pcsk9*$^{-/-}$ mice showed a significant accumulation of lipid droplets in hepatocytes and a ≈4-fold increase in triglyceride content (Figure 4E and 4F). In line with these results, acute injection of the fluorescent palmitate analog Bodipy FL $C_{16}$ to control +/+ and *Pcsk9*$^{-/-}$ mice revealed a 2-fold increase of fatty acid uptake by the liver in *Pcsk9*$^{-/-}$ mice (Figure 4G). Altogether, these results indicate that *Pcsk9*$^{-/-}$ mice have an altered hepatic fatty acid metabolism.

## Discussion

PCSK9 was shown to cause the post-translational degradation of LDLR and familial hypercholesterolemia >10 years ago, but its role in enhancing the degradation of other cell surface receptors is still emerging. In this work, we characterized a novel function of PCSK9 causing the degradation of CD36, a major receptor involved in fatty acid and triglyceride metabolism. Our results demonstrate that PCSK9 directly interacts with CD36 with a $K_d$ of 1.2 µmol/L, which is similar to its binding with the LDLR EGFA domain at neutral pH[24,25] and within the range of micromolar-binding affinity of other CD36 ligands.[23] Accordingly, we found that PCSK9 and CD36 coimmunoprecipitate and colocalize at the cell surface and in lysosomes either under overexpression or physiological conditions in hepatic and adipocyte cell lines. PCSK9 elicited the degradation of CD36 both through an intracellular or extracellular pathway and reduced the level of CD36 at the cell surface, likely by impeding the recycling or translocation of CD36 to the plasma membrane and directing the receptor to the lysosomes. Functionally, reduction of CD36 levels significantly decreased internalization of ligands, such as oxidized-LDL in hepatic cells and a palmitate analog in adipocytes. Conversely, CD36 protein levels were robustly increased, as well as that of LDLR, on small interfering RNA knockdown of *PCSK9* gene expression in HepG2-CD36 cells. In vivo, injection of recombinant PCSK9 to WT C57BL/6 mice induced hepatic CD36 degradation. Inversely, the absence of PCSK9 resulted in the strong upregulation of CD36 protein levels in the liver and adipose tissue and was associated with an increase in hepatic fatty acid uptake and triglyceride content.

The mechanism by which PCSK9 promotes CD36 degradation was evaluated and compared with that of LDLR. Our results show that inhibitors of proteasome (MG132, lactacystin, ALLN, and proteasome inhibitor-1) or lysosomes ($NH_4Cl$, E64D, and bafilomycin A1) prevented the PCSK9-induced destruction of CD36, which contrast with that of LDLR that is solely inhibited by lysosome inhibitors.[3,32] The inhibition of CD36 degradation by proteasome and lysosome inhibitors, added to the fact that degradation was prevented in brefeldin A–treated cells, might suggest the involvement of ubiquitin-mediated targeting of CD36 to lysosomes and the crosstalk between the ubiquitin–proteasome and autophagy–lysosome systems.[33] Indeed, the addition of ubiquitin tags to many cell surface receptors serve as a sorting signal to lysosomes.[34] Deubiquitination of endosomal CD36, which is required for trafficking to multivesicular bodies and lysosomes, may be mediated by the proteasome.[35] However, ubiquitin is essential for LDLR degradation by the inducible degrader of the LDLR, but not by PCSK9,[32] and if PCSK9 promotes CD36 ubiquitination remains to be demonstrated.

Binding of PCSK9 to LDLR requires key residues found on the surface of its catalytic domain.[26] Our results indicate that the same residues are not involved for PCSK9–CD36 complex formation. The PCSK9-D374Y mutant, which increases the affinity and degradation potency of PCSK9 toward LDLR,[11] did not increase CD36 degradation compared with WT PCSK9. In addition, the PCSK9-F379A mutant, which greatly diminishes binding to and degradation of LDLR,[26] coimmunoprecipitated with CD36 and induced its degradation with more potency than WT PCSK9. Although it is not excluded that LDLR may be involved in the trafficking of the CD36/PCSK9 complex, our data suggest that PCSK9-mediated CD36

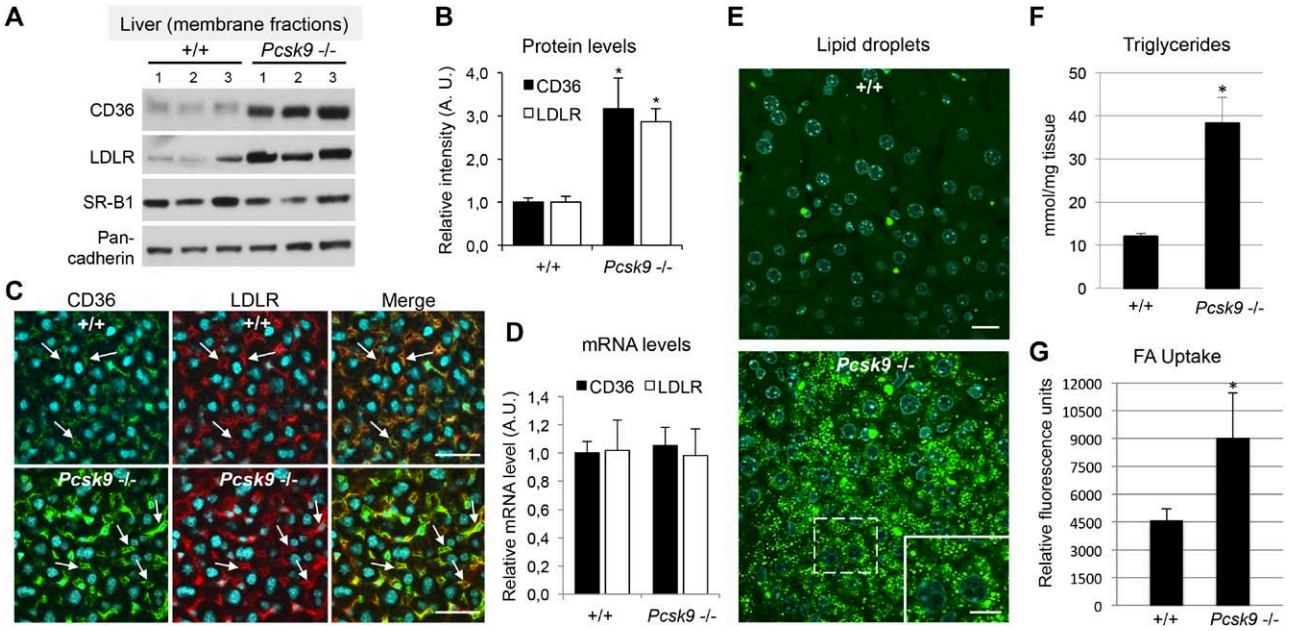


**Figure 4.** Proprotein convertase subtilisin/kexin type 9 (PCSK9) regulates hepatic cluster of differentiation 36 (CD36) protein levels, long-chain fatty acid uptake, and triglyceride content. **A**, Representative Western blotting (WB) of CD36, low-density lipoprotein receptor [LDLR], SR-B1, and pan-cadherin in mouse liver total membrane fractions from C57BL/6 (+/+) and *Pcsk9*$^{-/-}$ mice. **B**, Densitometric analysis of CD36 and LDLR WB signals normalized over that of pan-cadherin. (+/+, n=10 mice; *Pcsk9*$^{-/-}$, n=8 mice). **P*<0.001 vs the +/+ group. **C**, Immunofluorescence of CD36 (**left**) and LDLR (**middle**) in liver cryosections of +/+ and *Pcsk9*$^{-/-}$ mice. Colocalization (arrows) of CD36 with LDLR at the basolateral membrane of hepatocytes is exemplified by the yellow color in the merge image. Nuclei were stained with DAPI (cyan). Bars, 40 μm. **D**, Hepatic CD36 and LDLR mRNA levels as determined by quantitative polymerase chain reaction (+/+, n=13 mice; *Pcsk9*$^{-/-}$, n=10 mice). **E**, Confocal microscopy of cryosections of liver tissues from +/+ and *Pcsk9*$^{-/-}$ mice stained with Bodipy 493/503 (lipid droplets; green) and DAPI (nuclei; cyan). Bar, 20 μm. Inset bar, 10 μm. **F**, Hepatic triglyceride measurements from +/+ and *Pcsk9*$^{-/-}$ mice (+/+, n=12 mice; *Pcsk9*$^{-/-}$, n=11 mice). **P*<0.001 vs +/+. **G**, Liver fatty acid (FA) uptake measured after injection of Bodipy FL $C_{16}$ in +/+ or *Pcsk9*$^{-/-}$ mice as indicated in experimental procedures (+/+, n=3 mice; *Pcsk9*$^{-/-}$, n=3 mice). **P*<0.05 vs +/+.

degradation could occur in the absence of LDLR, as demonstrated previously for very low-density lipoprotein receptor, APOER2 (apolipoprotein E receptor 2), and CD81.[14,15] These results suggest that critical PCSK9 residues differ for LDLR and CD36 but that the catalytic domain (aa 153–421) affects binding to CD36. Indeed, we showed that a PCSK9 neutralizing antibody against the catalytic domain prevented CD36 degradation and LDLR. Similar to PCSK9-mediated LDLR degradation,[14,30] CD36 degradation is cell type and tissue dependent. Although the mechanism is still unclear, it has been proposed that inhibition of PCSK9 binding to LDLR by annexin A2 in extrahepatic tissues[36] or that PCSK9 dissociates from the LDLR within early endosomes[37] contribute to PCSK9 resistance. Whether this applies to CD36 remains to be demonstrated and, as for LDLR, the complete mechanism remains to be resolved. CD36 endocytosis can be mediated through clathrin-dependent or lipid raft pathways,[38] whereas LDLR endocytosis and degradation are clathrin dependent.[7,32] Therefore, PCSK9 could be internalized with CD36 through different endocytotic pathways and, in some cell types or tissues, this might not always result in degradation of the receptor. CD36 was resistant to PCSK9 in insulin-stimulated HL-1 cardiac muscle cells and in PMA-induced THP-1 macrophages, in conditions favoring CD36 translocation at the cell surface, as well as not regulated by PCSK9 in mouse heart and jejunum. In line with these results, it was shown that PCSK9 failed to induce the degradation of CD36 in polarized intestinal Caco-2 cells.[39] Moreover, through a yet undefined mechanism, the addition of PCSK9 to the basolateral medium of Caco-2 cells grown on filter inserts, which separates the basolateral and apical domain, increased the expression of CD36 and NPC1L1 at the apical surface resulting in enhanced cholesterol uptake and chylomicron secretion.[39] However, our results demonstrated that, independently of the nutritional status, apical CD36 levels were not overtly modified in the jejunum of *Pcsk9*$^{-/-}$ mice, suggesting that intestinal CD36 may not participate to the reduced postprandial hypertriglyceridemia phenotype of *Pcsk9*$^{-/-}$ mice.[19]

PCSK9-deficient mice have visceral fat accumulation (our unpublished observations).[40] This phenotype was shown to be LDLR independent and may be in part mediated by very low-density lipoprotein receptor. CD36 is a major regulator of adipose tissue growth and function; CD36 null mice are significantly leaner than WT mice and display increased plasma levels of triglyceride and fatty acids.[41] Our results demonstrate that CD36 level is regulated by PCSK9 in mouse primary adipocytes and 3T3-L1 adipocytes. In addition, CD36 protein level is increased by ≈80% in perigonadal fat pads of *Pcsk9*$^{-/-}$ mice, suggesting that it represents an important factor causing the increase in adiposity in *Pcsk9*$^{-/-}$ mice. Through an LDLR-independent mechanism, PCSK9 was shown to modulate hepatic and intestinal secretion and uptake of triglyceride-rich lipoproteins and postprandial triglyceride levels.[19,42] Herein, we show that CD36 levels were increased by ≈3-fold in the liver of *Pcsk9*$^{-/-}$ mice and, in accordance with the function of CD36 in fatty acid uptake, long-chain fatty acid analog

uptake, triglycerides, and lipid droplets were significantly increased in the liver of *Pcsk9*$^{-/-}$ mice. Unlike young ≈2- to 3-month-old *Pcsk9*$^{-/-}$ mice,[22] our experiments, conducted with ≈6- to 7-month-old mice, showed an increase in hepatic triglyceride content, suggesting that the long-term effect of elevated CD36 in the liver may result in accumulation of lipids.[21] Indeed, enhanced CD36-mediated hepatic fat uptake is associated with greater susceptibility to nonalcoholic fatty liver disease in mice and humans.[43] In addition, PCSK9 loss-of-function mutations, which can result in familial hypobetalipoproteinemia, could be a cause of mild fatty liver disease.[44] Whether this might occur after long-term inhibition of PCSK9 in humans remains to be evaluated.

In conclusion, we have demonstrated for the first time that PCSK9 induces the degradation of CD36 via a proteasome-sensitive mechanism in a post-endoplasmic reticulum, acidic compartment. PCSK9-mediated modulation of CD36 levels in tissues with important lipid fluxes, such as in the liver and visceral adipose tissue, may restrict fatty acid internalization and triglyceride storage and provide additional mechanistic support to the role of PCSK9 in triglyceride metabolism.

## Acknowledgments

We thank Nicolas Bousette and John D. Rioux at the Montreal Heart Institute for their generous gift of cell lines. We are also grateful to Steve Bourgault (Université du Québec à Montréal) for expert help with SPR analyses and to Catherine Martel (Montreal Heart Institute) for critical reading of the article.

## Sources of Funding

This work was supported by research grants from the Canadian Institutes of Health Research (CIHR—Institute of Nutrition, Metabolism and Diabetes; MOP133598), the Heart and Stroke Foundation of Canada, the Fonds de la Recherche en Santé du Québec, and the Montreal Heart Institute Foundation to Dr Mayer.

## Disclosures

None.

## References

1. Do R, Stitziel NO, Won HH, et al; NHLBI Exome Sequencing Project. Exome sequencing identifies rare LDLR and APOA5 alleles conferring risk for myocardial infarction. *Nature*. 2015;518:102–106. doi: 10.1038/nature13917.
2. Kotowski IK, Pertsemlidis A, Luke A, Cooper RS, Vega GL, Cohen JC, Hobbs HH. A spectrum of PCSK9 alleles contributes to plasma levels of low-density lipoprotein cholesterol. *Am J Hum Genet*. 2006;78:410–422. doi: 10.1086/500615.
3. Maxwell KN, Fisher EA, Breslow JL. Overexpression of PCSK9 accelerates the degradation of the LDLR in a post-endoplasmic reticulum compartment. *Proc Natl Acad Sci U S A*. 2005;102:2069–2074. doi: 10.1073/pnas.0409736102.
4. Abifadel M, Varret M, Rabès JP, et al. Mutations in PCSK9 cause autosomal dominant hypercholesterolemia. *Nat Genet*. 2003;34:154–156. doi: 10.1038/ng1161.
5. Timms KM, Wagner S, Samuels ME, Forbey K, Goldfine H, Jammulapati S, Skolnick MH, Hopkins PN, Hunt SC, Shattuck DM. A mutation in PCSK9 causing autosomal-dominant hypercholesterolemia in a Utah pedigree. *Hum Genet*. 2004;114:349–353. doi: 10.1007/s00439-003-1071-9.
6. Cohen JC, Boerwinkle E, Mosley TH Jr, Hobbs HH. Sequence variations in PCSK9, low LDL, and protection against coronary heart disease. *N Engl J Med*. 2006;354:1264–1272. doi: 10.1056/NEJMoa054013.
7. Poirier S, Mayer G. The biology of PCSK9 from the endoplasmic reticulum to lysosomes: new and emerging therapeutics to control low-density lipoprotein cholesterol. *Drug Des Devel Ther*. 2013;7:1135–1148. doi: 10.2147/DDDT.S36984.
8. Seidah NG, Benjannet S, Wickham L, Marcinkiewicz J, Jasmin SB, Stifani S, Basak A, Prat A, Chretien M. The secretory proprotein convertase neural apoptosis-regulated convertase 1 (NARC-1): liver regeneration and neuronal differentiation. *Proc Natl Acad Sci U S A*. 2003;100:928–933. doi: 10.1073/pnas.0335507100.
9. Mayer G, Poirier S, Seidah NG. Annexin A2 is a C-terminal PCSK9-binding protein that regulates endogenous low density lipoprotein receptor levels. *J Biol Chem*. 2008;283:31791–31801. doi: 10.1074/jbc.M805971200.
10. Mayer G, Hamelin J, Asselin MC, Pasquato A, Marcinkiewicz E, Tang M, Tabibzadeh S, Seidah NG. The regulated cell surface zymogen activation of the proprotein convertase PC5A directs the processing of its secretory substrates. *J Biol Chem*. 2008;283:2373–2384. doi: 10.1074/jbc.M708763200.
11. Cunningham D, Danley DE, Geoghegan KF, et al. Structural and biophysical studies of PCSK9 and its mutants linked to familial hypercholesterolemia. *Nat Struct Mol Biol*. 2007;14:413–419. doi: 10.1038/nsmb1235.
12. McNutt MC, Lagace TA, Horton JD. Catalytic activity is not required for secreted PCSK9 to reduce low density lipoprotein receptors in HepG2 cells. *J Biol Chem*. 2007;282:20799–20803. doi: 10.1074/jbc.C700095200.
13. Zhang DW, Lagace TA, Garuti R, Zhao Z, McDonald M, Horton JD, Cohen JC, Hobbs HH. Binding of proprotein convertase subtilisin/kexin type 9 to epidermal growth factor-like repeat A of low density lipoprotein receptor decreases receptor recycling and increases degradation. *J Biol Chem*. 2007;282:18602–18612. doi: 10.1074/jbc.M702027200.
14. Poirier S, Mayer G, Benjannet S, Bergeron E, Marcinkiewicz J, Nassoury N, Mayer H, Nimpf J, Prat A, Seidah NG. The proprotein convertase PCSK9 induces the degradation of low density lipoprotein receptor (LDLR) and its closest family members VLDLR and ApoER2. *J Biol Chem*. 2008;283:2363–2372. doi: 10.1074/jbc.M708098200.
15. Labonté P, Begley S, Guévin C, Asselin MC, Nassoury N, Mayer G, Prat A, Seidah NG. PCSK9 impedes hepatitis C virus infection *in vitro* and modulates liver CD81 expression. *Hepatology*. 2009;50:17–24. doi: 10.1002/hep.22911.
16. Sharotri V, Collier DM, Olson DR, Zhou R, Snyder PM. Regulation of epithelial sodium channel trafficking by proprotein convertase subtilisin/kexin type 9 (PCSK9). *J Biol Chem*. 2012;287:19266–19274. doi: 10.1074/jbc.M112.363382.
17. Jonas MC, Costantini C, Puglielli L. PCSK9 is required for the disposal of non-acetylated intermediates of the nascent membrane protein BACE1. *EMBO Rep*. 2008;9:916–922. doi: 10.1038/embor.2008.132.
18. Lakoski SG, Lagace TA, Cohen JC, Horton JD, Hobbs HH. Genetic and metabolic determinants of plasma PCSK9 levels. *J Clin Endocrinol Metab*. 2009;94:2537–2543. doi: 10.1210/jc.2009-0141.
19. Le May C, Kourimate S, Langhi C, Chétiveaux M, Jarry A, Comera C, Collet X, Kuipers F, Krempf M, Cariou B, Costet P. Proprotein convertase subtilisin kexin type 9 null mice are protected from postprandial triglyceridemia. *Arterioscler Thromb Vasc Biol*. 2009;29:684–690. doi: 10.1161/ATVBAHA.108.181586.
20. Silverstein RL, Febbraio M. CD36, a scavenger receptor involved in immunity, metabolism, angiogenesis, and behavior. *Sci Signal*. 2009;2:re3. doi: 10.1126/scisignal.272re3.
21. Koonen DP, Jacobs RL, Febbraio M, Young ME, Soltys CL, Ong H, Vance DE, Dyck JR. Increased hepatic CD36 expression contributes to dyslipidemia associated with diet-induced obesity. *Diabetes*. 2007;56:2863–2871. doi: 10.2337/db07-0907.
22. Rashid S, Curtis DE, Garuti R, Anderson NN, Bashmakov Y, Ho YK, Hammer RE, Moon YA, Horton JD. Decreased plasma cholesterol and hypersensitivity to statins in mice lacking Pcsk9. *Proc Natl Acad Sci U S A*. 2005;102:5374–5379. doi: 10.1073/pnas.0501652102.
23. Bolduc OR, Lambert-Lanteigne P, Colin DY, Zhao SS, Proulx C, Boeglin D, Lubell WD, Pelletier JN, Féthière J, Ong H, Masson JF. Modified peptide monolayer binding His-tagged biomolecules for small ligand screening with SPR biosensors. *Analyst*. 2011;136:3142–3148. doi: 10.1039/c1an15235a.
24. Shan L, Pang L, Zhang R, Murgolo NJ, Lan H, Hedrick JA. PCSK9 binds to multiple receptors and can be functionally inhibited by an EGF-A peptide. *Biochem Biophys Res Commun*. 2008;375:69–73. doi: 10.1016/j.bbrc.2008.07.106.
25. Fisher TS, Lo Surdo P, Pandit S, et al. Effects of pH and low density lipoprotein (LDL) on PCSK9-dependent LDL receptor regulation. *J Biol Chem*. 2007;282:20502–20512. doi: 10.1074/jbc.M701634200.

26. Kwon HJ, Lagace TA, McNutt MC, Horton JD, Deisenhofer J. Molecular basis for LDL receptor recognition by PCSK9. *Proc Natl Acad Sci U S A*. 2008;105:1820–1825. doi: 10.1073/pnas.0712064105.
27. Tran TT, Poirier H, Clément L, Nassir F, Pelsers MM, Petit V, Degrace P, Monnot MC, Glatz JF, Abumrad NA, Besnard P, Niot I. Luminal lipid regulates CD36 levels and downstream signaling to stimulate chylomicron synthesis. *J Biol Chem*. 2011;286:25201–25210. doi: 10.1074/jbc.M111.233551.
28. Luiken JJ, Dyck DJ, Han XX, Tandon NN, Arumugam Y, Glatz JF, Bonen A. Insulin induces the translocation of the fatty acid transporter FAT/CD36 to the plasma membrane. *Am J Physiol Endocrinol Metab*. 2002;282:E491–E495. doi: 10.1152/ajpendo.00419.2001.
29. Longva KE, Blystad FD, Stang E, Larsen AM, Johannessen LE, Madshus IH. Ubiquitination and proteasomal activity is required for transport of the EGF receptor to inner membranes of multivesicular bodies. *J Cell Biol*. 2002;156:843–854. doi: 10.1083/jcb.200106056.
30. Grefhorst A, McNutt MC, Lagace TA, Horton JD. Plasma PCSK9 preferentially reduces liver LDL receptors in mice. *J Lipid Res*. 2008;49:1303–1311. doi: 10.1194/jlr.M800027-JLR200.
31. Matter K, Hunziker W, Mellman I. Basolateral sorting of LDL receptor in MDCK cells: the cytoplasmic domain contains two tyrosine-dependent targeting determinants. *Cell*. 1992;71:741–753.
32. Wang Y, Huang Y, Hobbs HH, Cohen JC. Molecular characterization of proprotein convertase subtilisin/kexin type 9-mediated degradation of the LDLR. *J Lipid Res*. 2012;53:1932–1943. doi: 10.1194/jlr.M028563.
33. Korolchuk VI, Menzies FM, Rubinsztein DC. Mechanisms of cross-talk between the ubiquitin-proteasome and autophagy-lysosome systems. *FEBS Lett*. 2010;584:1393–1398. doi: 10.1016/j.febslet.2009.12.047.
34. Miranda M, Sorkin A. Regulation of receptors and transporters by ubiquitination: new insights into surprisingly similar mechanisms. *Mol Interv*. 2007;7:157–167. doi: 10.1124/mi.7.3.7.
35. Smith J, Su X, El-Maghrabi R, Stahl PD, Abumrad NA. Opposite regulation of CD36 ubiquitination by fatty acids and insulin: effects on fatty acid uptake. *J Biol Chem*. 2008;283:13578–13585. doi: 10.1074/jbc.M800008200.
36. Seidah NG, Poirier S, Denis M, Parker R, Miao B, Mapelli C, Prat A, Wassef H, Davignon J, Hajjar KA, Mayer G. Annexin A2 is a natural extrahepatic inhibitor of the PCSK9-induced LDL receptor degradation. *PLoS One*. 2012;7:e41865. doi: 10.1371/journal.pone.0041865.
37. Nguyen MA, Kosenko T, Lagace TA. Internalized PCSK9 dissociates from recycling LDL receptors in PCSK9-resistant SV-589 fibroblasts. *J Lipid Res*. 2014;55:266–275. doi: 10.1194/jlr.M044156.
38. Heit B, Kim H, Cosío G, Castaño D, Collins R, Lowell CA, Kain KC, Trimble WS, Grinstein S. Multimolecular signaling complexes enable Syk-mediated signaling of CD36 internalization. *Dev Cell*. 2013;24:372–383. doi: 10.1016/j.devcel.2013.01.007.
39. Levy E, Ben Djoudi Ouadda A, Spahis S, Sane AT, Garofalo C, Grenier É, Emonnot L, Yara S, Couture P, Beaulieu JF, Ménard D, Seidah NG, Elchebly M. PCSK9 plays a significant role in cholesterol homeostasis and lipid transport in intestinal epithelial cells. *Atherosclerosis*. 2013;227:297–306. doi: 10.1016/j.atherosclerosis.2013.01.023.
40. Roubtsova A, Munkonda MN, Awan Z, Marcinkiewicz J, Chamberland A, Lazure C, Cianflone K, Seidah NG, Prat A. Circulating proprotein convertase subtilisin/kexin 9 (PCSK9) regulates VLDLR protein and triglyceride accumulation in visceral adipose tissue. *Arterioscler Thromb Vasc Biol*. 2011;31:785–791. doi: 10.1161/ATVBAHA.110.220988.
41. Febbraio M, Abumrad NA, Hajjar DP, Sharma K, Cheng W, Pearce SF, Silverstein RL. A null mutation in murine CD36 reveals an important role in fatty acid and lipoprotein metabolism. *J Biol Chem*. 1999;274:19055–19062.
42. Tavori H, Fan D, Blakemore JL, Yancey PG, Ding L, Linton MF, Fazio S. Serum proprotein convertase subtilisin/kexin type 9 and cell surface low-density lipoprotein receptor: evidence for a reciprocal regulation. *Circulation*. 2013;127:2403–2413. doi: 10.1161/CIRCULATIONAHA.113.001592.
43. Sheedfar F, Sung MM, Aparicio-Vergara M, Kloosterhuis NJ, Miquilena-Colina ME, Vargas-Castrillón J, Febbraio M, Jacobs RL, de Bruin A, Vinciguerra M, García-Monzón C, Hofker MH, Dyck JR, Koonen DP. Increased hepatic CD36 expression with age is associated with enhanced susceptibility to nonalcoholic fatty liver disease. *Aging (Albany NY)*. 2014;6:281–295.
44. Cariou B, Le May C, Costet P. Clinical aspects of PCSK9. *Atherosclerosis*. 2011;216:258–265. doi: 10.1016/j.atherosclerosis.2011.04.018.




## Significance

Proprotein convertase subtilisin/kexin type 9 (PCSK9) reduces the protein levels of low-density lipoprotein receptor that is essential for clearance of atherogenic low-density lipoprotein cholesterol from the bloodstream. Accordingly, the use of PCSK9 inhibitors aimed at reducing hypercholesterolemia could prevent major cardiovascular events. However, the mechanism by which PCSK9 regulates triglyceride metabolism is not well understood. Herein, we provide evidence that PCSK9 induces the degradation of CD36, a major receptor for long-chain fatty acids. Our results show that PCSK9 regulates CD36 protein levels and function in vitro in hepatic and adipose cell lines, ex vivo in primary adipocytes, and in vivo in visceral adipose tissue and liver of mice. Importantly, our data show that the absence of PCSK9 causes increased hepatic fatty acid uptake and triglyceride storage, likely through CD36 upregulation. These data support that PCSK9-induced CD36 degradation may serve to limit the entry of fatty acids and triglyceride accumulation in tissues, such as the liver.

Arteriosclerosis, Thrombosis, and Vascular Biology

JOURNAL OF THE AMERICAN HEART ASSOCIATION



# PCSK9 Induces CD36 Degradation and Affects Long-Chain Fatty Acid Uptake and Triglyceride Metabolism in Adipocytes and in Mouse Liver

Annie Demers, Samaneh Samami, Benjamin Lauzier, Christine Des Rosiers, Emilienne Tudor Ngo Sock, Huy Ong and Gaetan Mayer

*Arterioscler Thromb Vasc Biol.* 2015;35:2517-2525; originally published online October 22, 2015;
doi: 10.1161/ATVBAHA.115.306032
*Arteriosclerosis, Thrombosis, and Vascular Biology* is published by the American Heart Association, 7272 Greenville Avenue, Dallas, TX 75231

Print ISSN: 1079-5642. Online ISSN: 1524-4636

# SUPPLEMENTAL MATERIAL

# PCSK9 induces CD36 degradation and impacts long-chain fatty acid uptake and triglyceride metabolism in adipocytes and in mouse liver

Annie Demers, Samaneh Samami, Benjamin Lauzier, Christine Des Rosiers, Emilienne Ngo Sock, Huy Ong, Gaétan Mayer

## METHODS

### Expression Constructs

The open reading frame corresponding to human CD36 (clone ID 4244251, Open Biosystems) was PCR-amplified and subcloned into BglII/AgeI-digested pIRES2-EGFP vector (Invitrogen) with either a C-terminal V5 or human influenza hemagglutinin (HA) epitope tag (YPYDVPDYA). The cDNAs encoding for full-length wild-type human PCSK9, PCSK5 (PC5A) and furin, with or without a C-terminal V5 tag, were cloned into pIRES2-EGFP as described previously[1]. Human proprotein convertase subtilisin kexin isozyme-1 (SKI-1; (*MBTPS1*) clone ID 40054074, Open Biosystem) was fused in frame with the C-terminal V5 tag and inserted into pIRES2-EGFP using NheI/AgeI. Human LIMP2 cDNA (clone ID HsCD00002469, DNASU) was PCR-amplified and subcloned into NheI/AgeI-digested pIRES2-EGFP with a C-terminal HA tag. The pIRES-PCSK9-D374Y-V5 and pIRES-PCSK9-F379A-V5 mutant constructs were generated by PCR mutagenesis using the pIRES-PCSK9-V5 cDNA template. PCSK9-mCherry was constructed by fusing monomeric fluorescent Cherry (mCherry) coding cDNA to PCSK9 C-terminus using pCMV-Cav1-mCherry as a template (Cat. #27705, Addgene). Prior to subcloning human PCSK9 in frame at the AgeI cloning site, one nucleotide deletion was performed by QuickChange II site-directed mutagenesis using the following oligonucleotides: 5'-

CAGACCGGTCGCCACATGGTGAGCAAGG; 5'-CCTTGCTCACCATGTGGCGACCGGTCTG. The caveolin-1 cassette was then replaced by human PCSK9 cDNA at the BglII/AgeI cloning sites. Plasmid encoding the C-terminal hexahistidine-tagged PCSK9 (pIRES-PCSK9-V5-$His_6$) was generated by overlapping PCR. Human CD36 ectodomain (hCD36ED; aa 30-439) was amplified by PCR from pcDNA3.1+hCD36 (kindly provided by M. Febbraio, University of Alberta, Alberta) and subcloned into a modified pFastBac1 transfer plasmid (pKMJ-His3C, kindly provided by M. Jinek, University of California, Berkeley) carrying an N-terminal viral signal sequence, a Flag epitope (DYKDDDDK) and a hexahistidine tag. Recombinant baculovirus was produced using the standard Bac-to-Bac protocol (Invitrogen) according to the manufacturer. All cDNA constructs were verified by DNA sequencing.

**Antibodies**

The rabbit polyclonal antibody against human PCSK9 (anti-hPCSK9) was produced in our laboratory as previously described[1]. The neutralizing anti-human PCSK9 monoclonal antibody was from BPS Bioscience. Goat polyclonals against mouse CD36 (anti-mCD36), mouse LDLR (anti-mLDLR) and human LDLR (anti-hLDLR), and mouse monoclonal anti-His tag antibody were from R&D Systems. Mouse anti-V5-HRP, rabbit anti-actin and rabbit anti-HA tag antibodies were purchased from Sigma. Unconjugated mouse anti-V5 antibody was from Invitrogen, rabbit anti-mouse LDLR, anti-mouse SRB1 and anti-human CD36 (anti-hCD36) antibodies were from Novus Biologicals and rabbit anti-pan-Cadherin from Life Technologies. Mouse anti-mannose 6-phosphate receptor (M6PR) antibody (cation independent, clone 2G11) was from Abcam.

**Recombinant Proteins**

For recombinant human PCSK9 (rhPCSK9; aa 31-692) production, HEK293T cells (20 x 75 $cm^2$) were transfected with pIRES-PCSK9-V5-$His_6$ to produce ~1 L of conditioned medium. The medium was supplemented with 5 mM imidazole, filtered (0.45 µm), and applied onto a pre-equilibrated (Buffer A; 20 mM sodium phosphate pH 7.4 and 500 mM NaCl) HisTRAP excel column (GE Healthcare), using an AKTA fast-performance liquid chromatography system (GE

Healthcare) maintained at 4°C. The column was then washed with 15 bed volumes of Buffer A containing 5 mM imidazole and recombinant PCSK9 was eluted with 10 bed volumes of a linear imidazole gradient (5 to 500 mM). Absorbance at 280 nm, SDS-PAGE/Coomassie staining and Western blotting (WB) (see below) using the anti-hPCSK9 antibody were used to identify rhPCSK9-enriched fractions. The latter were pooled, concentrated to 120 µl using Amicon centrifugal filters 3 kDa cut-off (Millipore) and subjected to size-exclusion chromatography on a Superose 12 10/300 GL column (GE Healthcare) equilibrated with 25 mM HEPES pH 7.4 and 150 mM NaCl. Protein purity and identity were confirmed by SDS-PAGE and Coomassie staining as well as WB. PCSK9 concentration was determined by ELISA (Circulex).

Recombinant human CD36 ectodomain (hCD36ED) was expressed as a secreted protein in *Trichoplusia ni* High Five insect cells. Protein expression was achieved by infecting 3 L of shaking culture cells at a density of 2 x $10^6$ cells/ml with the recombinant baculovirus bearing the cDNA coding for hCD36ED-Flag-$His_6$ at an MOI of 3. After 72 h post-infection, the conditioned medium was cleared of cells by centrifugation (10,000 x g for 30 min) and diafiltered by tangential flow ultrafiltration using a 30 kDa cut-off cartridge (Pall) in binding buffer (50 mM Tris pH 8.0, 500 mM NaCl, 1 mM PMSF) at 4 $^oC$. The recombinant hCD36ED was first purified by $Ni^{2+}$ affinity chromatography on a Poros perfusion chromatography column (Applied Biosystems) pre-equilibrated with binding buffer. After extensive washing, the protein was eluted with a 0-500 mM imidazole gradient in 50 mM Tris pH 8.0, 150 mM NaCl and 1 mM PMSF. Fractions were analyzed by WB using the anti-hCD36 antibody. Positive fractions were pooled and dialyzed in 50 mM Tris pH 8.0 containing 150 mM NaCl for immunoaffinity purification on an anti-flag M2 affinity gel (Sigma). The protein was eluted with 0.1 M glycine buffer pH 3.5 and neutralized in 1M Tris-HCl buffer pH 8. Fractions were analyzed by WB using the anti-hCD36 antibody. Fractions containing purified hCD36ED protein were pooled and concentrated on a 30 kDa cut-off Amicon Ultracel centrifugal filter unit (Millipore).

**Surface plasmon resonance (SPR) analysis**

SPR analyses were performed using a Biacore T200 instrument (*GE Healthcare*). hCD36ED recombinant protein was immobilized on a carboxymethylated dextran CM5 sensor chip (GE Healthcare) using an amine-coupling strategy. Briefly, the sensor chip surface was activated with a 1:1 mixture of N-hydroxysuccinimide and 3-(N,Ndimethylamino)-propyl-N-ethylcarbondiimide. hCD36ED solution (15 mg/mL solubilized in acetate buffer pH 6) was injected at a flow rate of 10 ml/min using HBS-N running buffer (10 mM HEPES, 150 mM NaCl, pH 7.4) to reach a level of immobilization of 100 RU. Surfaces (protein and reference) were blocked by the injection of an ethanolamine solution. Binding kinetics of PCSK9 over the CD36 sensor chip was evaluated in 25 mM HEPES buffer (150 mM NaCl, 1 mM CaCl2, pH 7.4) at increased concentrations (0.05 to 2 µM) at a flow rate of 20 ml/min. The sensor chip was regenerated by injecting 15 ml of a 10 mM glycine solution, pH 2.5. Binding sensograms were obtained by subtraction of the reference flow cell. Data analysis was performed using the BIAevaluation software package (*GE Healthcare*).

**Cell Culture, Transfections and Cell Treatments**

HEK293 and HepG2 cells were grown in DMEM supplemented with 10% fetal bovine serum (FBS) (Wisent) and transfected using Effectene (Qiagen) and FUGENE HD (Promega), respectively, according to the manufacturer's instructions. Stable transfectants of pIRES-hCD36-HA were obtained in HepG2 cells following G418 selection. Mouse 3T3-L1 preadipocytes, a kind gift of J-F Tanguay (Montreal Heart Institute (MHI), Montreal), were grown in DMEM supplemented with 10% fetal calf serum (FCS). Two day post-confluent 3T3-L1 cells (day 0) were induced to differentiate into adipocytes by incubation in DMEM containing 10% FBS, 0.5 mM 3-isobutyl-1-methylxanthine (IBMX), 1 µM dexamethasone and 167 nM insulin (all from Sigma-Aldrich) for 2 days. The medium was then replaced with DMEM/10% FBS containing 167 nM insulin for another 2 days. Afterward, cells were refed with fresh DMEM/10% FBS every 2 days and used for experiments between day 8 and day 12 post-differentiation. THP-1

monocytes (kindly provided by J. Rioux, MHI) were grown in RPMI 1640 medium (Wisent) containing 10% FBS and 50 µM 2-mercaptoethanol and macrophage differentiation was induced by addition of 5 ng/ml phorbol 12-myristate 13-acetate (PMA, Sigma-Aldrich) for 72 h. HL-1 mouse cardiomyocytes (kindly provided by N. Bousette, MHI) were cultured in Claycomb medium (Sigma-Aldrich) supplemented with 10% FCS, 0.1 mM norepinephrine (Sigma-Aldrich) and 2 mM L-glutamine. Cells were incubated for 16 h with 167 nM insulin to induce CD36 translocation to the plasma membrane[2].

Cells, nontransfected or 24 h post-transfection, were washed and incubated at 37°C either with conditioned medium of HEK293 cells overexpressing an empty vector (pIRES-V5), WT PCSK9-V5 or PCSK9-D374Y-V5 (secreted PCSK9, sPCSK9 ~2 µg/ml as determined by ELISA (Circulex)) or with serum-free medium supplemented with purified rhPCSK9, as indicated in the figure legends, for 16 h before cell surface biotinylation and/or medium collection and cell lysis as described below. Inhibition of the PCSK9-induced CD36 degradation was performed by incubating cells either with proteasome inhibitors (5 µM Proteasome Inhibitor I (PI-1), 20 µM N-Acetyl-Leu-Leu-Nle-CHO (ALLN), 20 µM lactacystin, or MG-132 (2.5 µM or 1 µM, as indicated in figure legends) (EMD Millipore)), the endosome/lysosome neutralizing agent ammonium chloride ($NH_4Cl$; 10 mM) (Sigma), the lysosomal cysteine proteases inhibitor E64D (10 uM; Enzo Life Sciences), bafilomycin A1 (lysosome inhibitor specific for vacuolar type H+-ATPase (V-ATPase) (100 nM; Sigma), the neutralizing anti-PCSK9 antibody (20 nM; pre-incubated with sPCSK9-V5 for 1 h at 4ºC prior incubation with cells) or the inhibitor of protein transport from the endoplasmic reticulum to the Golgi apparatus brefeldin A (BFA; 5 µg/ml) (MP Biochemical), for 16 h.

Following treatments, conditioned media were collected, cells were washed with ice-cold phosphate-buffered saline (PBS) and whole cell extracts were prepared using ice-cold radio-immunoprecipitation assay lysis buffer (RIPA, 50 mM Tris-HCl, pH 8, 150 mM NaCl, 1% Nonidet P-40, 0.1% SDS, 0.5% sodium deoxycholate) containing a cocktail of protease inhibitors (Roche

Applied Science). Cell lysates were clarified by centrifugation at 14,000 g (15 min at 4 °C) and the protein concentration was determined by Bradford assay (BioRad) before WB analyses.

**siRNA Transfection**

Stable HepG2-hCD36-HA cells were transfected with a siRNA targeting PCSK9 (Ambion, *Silencer*® Select 4390825), or a siGENOME non-targeting (NT) siRNA pool (Dharmacon) using Lipofectamine RNAiMAX (Life Technologies) according to the manufacturer's recommendations. Seventy-two hours post-transfection, cells were serum starved overnight before cell lysis in RIPA buffer as described above. HEK293 cells were transfected with a siRNA targeting LDLR (Qiagen Hs_LDLR_2) or the NT siRNA and, 48 h later, cells were co-transfected with CD36-HA and either with the control pIRES-V5 or pIRES-PCSK9-V5 plasmid for 24 h before cell lysis in RIPA buffer.

**Cell Surface Biotinylation, Immunoprecipitation, and Western Blotting**

For biochemical detection of CD36 at the plasma membrane, cells were washed with ice-cold PBS adjusted to pH 8.0 and biotinylated with 2 mM sulfosuccinimidyl-6-(biotin-amido)hexanoate (sulfo-NHS-LC-biotin, Pierce) for 30 min at 4°C. Cells were then washed with 100 mM glycine in PBS pH 8.0 to quench the reaction. Cells were lysed as described above and incubated with streptavidin-agarose beads (Santa Cruz Biotechnologies) overnight at 4°C. For immunoprecipitation experiments, cell lysates were pre-cleared with protein A/G-agarose beads (Santa Cruz) for 1 h at 4°C. Immunoprecipitation was carried out using goat anti-mCD36 (1:200; IP:CD36), anti-V5 (1:200; IP:V5) or anti-HA (1:500; IP:HA) antibodies and protein A/G-agarose beads with end-over-end rotation overnight at 4°C. Bead-captured proteins were washed five times with RIPA buffer and analyzed by WB.

For immunoblotting, media (10 µl), tissue (see below) and cell lysates (30 µg) or immunoprecipitated proteins were boiled for 5 min in reducing Laemmli sample buffer and resolved on 8% glycine SDS-PAGE gels. The size-separated proteins were transferred to nitrocellulose membranes, blocked for 1 h with 5% skimmed milk in 25 mM Tris-HCl pH 7.4, 150

mM NaCl and 0.05% Tween-20 (TBST), and then incubated overnight at 4°C with antibodies diluted in TBST-1% skimmed milk. Proteins were probed using the anti-V5-HRP (1:5000), anti-HA (1:5000), anti-mouse or human CD36 (1:2000), anti-PCSK9 (1:2000), anti-mouse or human LDLR (1:2000), anti-SRB1 (1:5000), anti-pan-Cadherin (1:1000), anti-β-actin (1:2000) antibodies and revealed using the appropriate HRP-conjugated secondary antibodies (1:10,000, GE Healthcare) followed by enhanced chemiluminescence. Blots were exposed to BioFlex films (InterScience) and quantification of band intensity was achieved with the ImageJ software and normalized to β-actin levels.

**Immunocytochemistry and Fluorescent Lipid Uptake**

For colocalization experiments, HEK293 cells were seeded in 35 mm glass-bottom culture dishes (MAtTek Corp) coated with 50 µg/ml laminin (Sigma) and co-transfected 24 h after with pIRES-PCSK9-V5 and pIRES-CD36-HA or with a 2:1:1 ratio of pIRES-PCSK9:pIRES-CD36-V5:pIRES-LIMP2-HA cDNA plasmids. Twenty-four hours post-transfection, cells were serum starved in presence of 2.5 µM MG132 for 16 h before proceeding to immunofluorescence as described below. Stable HepG2-CD36-HA cells were plated in 35 mm glass-bottom culture dishes and either left untransfected or transfected the following day with pIRES-PCSK9-V5. Twenty-four hours post-transfection, cells serum starved for 1 h before incubation with 10 µg/ml 1,1'-dioctadecyl-3,3,3',3'-tetramethylindocarbocyanine perchlorate (DiI)-oxidized LDL (DiI-oxLDL, Biomedical Technologies) for 1 h at 37°C. For long-chain fatty acid uptake, 3T3-L1 adipocytes grown and differentiated on 35 mm glass-bottom dishes were incubated with conditioned medium of HEK293 cells overexpressing either an empty vector (pIRES-V5) or PCSK9-V5 for 16h prior to incubation with 1 µM Bodipy-conjugated palmitate (Bodipy FL $C_{16}$, Life Technologies) for 30 min. Cell surface labelings were made under nonpermeabilizing conditions by fixation with 3.5% paraformaldehyde for 10 min at room temperature. For intracellular immunolabelings, cells were fixed with 3.5% paraformaldehyde and permeabilized in 0.1% Triton-X 100 for 15 min. Cells were then incubated with 1% bovine serum albumin for 30

min and with the indicated primary antibody; anti-mCD36 (1:200), anti-hPCSK9 (1:200), anti-M6PR (1:200), anti-V5 (1:500) or anti-HA (1:500) antibodies overnight at 4°C. Following four washes with PBS, cells were incubated for 1 h with corresponding species-specific Alexa fluor (488, 555, or 647)-tagged secondary antibodies (1:500; Invitrogen), then washed with PBS and covered with 90% glycerol supplemented with 5% diazabicyclo[2.2.2]octane (DABCO, Sigma). Cells were examined using an Olympus Fluoview FV10i confocal microscope. The colocalization coefficient between CD36 and PCSK9 or CD36 and M6PR was measured by selecting the entire cell and estimating the Pearson's correlation coefficient (r) value using ImageJ colocalization plugin (NIH). For colocalization of CD36 and PCSK9 in lysosomes of 3T3-L1 adipocytes, cells were grown and differentiated on 35 mm glass-bottom dishes and incubated with the goat anti-mCD36 and Alexa Fluor 647-conjugated anti-goat antibodies together with sPCSK9-mCherry (conditioned medium of HEK293 cells overexpressing PCSK9-mCherry) for 16h in the presence of 2.5 μM MG132 and 5 mM $NH_4Cl$ prior addition of 500 nM LysoTracker® Blue DND-22 (Life Technologies) for 2h. Live cells were then washed with DMEM without phenol red and examined using an Olympus Fluoview FV10i confocal microscope. Omission of the primary goat anti-mCD36 antibody was used as a negative control.

**Animal Experimentation**

C57BL/6 (wild-type, WT) and *Pcsk9* knockout (*Pcsk9*$^{-/-}$) mice were obtained from The Jackson Laboratory and bred at our facility. Animals were housed in a pathogen-free environment under 12 h light-dark cycles with free access to water and to standard chow diet. Unless stated otherwise, experiments were carried out on 24-28 week-old male and female mice. Mice were euthanized and perigonadal fat pads and livers were collected immediately after for protein and/or mRNA expression analyses. Perigonadal fat pads were dissected and homogenized in ice-cold RIPA buffer using a polytron tissue grinder. For crude liver membrane preparation, livers were frozen and pulverized under liquid nitrogen with a pre-chilled mortar and pestle. Liver powders were suspended in ice-cold homogenization buffer (20 mM Tris (pH 7.4), 5 mM EDTA,

250 mM sucrose, and protease inhibitor cocktail) and homogenized using a Dounce homogenizer. Liver homogenates were centrifuged at 1000 g for 10 min, and the resulting supernatants were centrifuged at 110,000 g for 75 min at 4°C. Pellets containing the membrane fraction were resuspended in solubilization buffer (50 mM Tris (pH 7.4), 100 mM NaCl, 50 mM LiCl, 5 mM EDTA, 0.5% (v/v) Triton X-100, 0.5% (w/v) sodium deoxycholate, 0.05% (w/v) SDS, 0.02% (w/v) sodium azide and protease inhibitor cocktail), incubated for 30 min on ice and clarified at 14,000 g for 10 min at 4°C. For *in vivo* CD36 degradation experiments, mice were injected into the tail vein with 0.9% NaCl (saline) or 32 µg rhPCSK9. Sixty (60) or 120 min after injection, mice were euthanized and the liver was removed for WB analysis. All experiments were performed in accordance with the Canadian Council on Animal Care guidelines and approved by the Montreal Heart Institute Animal Care Committee.

**Isolation and culture of primary adipose cells**

Ten (10) to 12-week-old male C57BL/6 mice were anesthetized and fat pads were removed and minced in isolation media (DMEM containing 1.5% BSA, 1% penicillin/streptomycin and 50 µg/mL gentamicin). Adipose tissue (1g) was digested in 5 mL of isolation media containing 1.25 mg/mL collagenase type II (Sigma) for 1h at 37°C. The suspension was filtered through a 100-µm nylon mesh and centrifuged at 500 g for 5 min. The adipocytes were gently recovered and washed once with culture medium (DMEM supplemented with 1% FBS, 1% pen/strep and 50 ug/mL gentamicin). The adipocytes were then plated in 12-well culture plates and incubated overnight with sPCSK9 before lysis in RIPA buffer.

**In vivo hepatic LCFA uptake assay**

Mice were fasted overnight and were injected i.p. with 20 µM Bodipy FL $C_{16}$ in 200 µl saline. Mice were euthanized 20 minutes after the injection and livers were harvested and homogenized in RIPA buffer containing protease inhibitors. Lipids were extracted by mixing lysates with 3 volumes of Dole's reagent (heptane: 2-propanol: 2 N sulfuric acid; 10:40:1, v/v/v) followed by centrifugation at 18,000 g for 10 min. The clear organic-phase supernatant (top layer) was

collected and 50 µl of the latter was added to a 96-well plate. Fluorescence was determined using a 488 nm excitation, 515 nm emission filter set (Biotek). Fluorescence units were normalized to the protein concentration of liver extracts.

**Measurement of Hepatic Triglycerides**

Snap-frozen liver pieces (25 mg) were homogenized in 500 µl of 5% (w/v) NP-40 in water, heated to 85°C in a water bath for 2-4 min until NP-40 appeared cloudy, and cooled down to room temperature. Heating and cooling steps were repeated once and samples were centrifuged at 14,000 g for 2 min to remove insoluble material. Total triglyceride concentrations were measured using a colorimetric assay kit (Abcam) following the manufacturer's protocol.

**Immunohistochemistry and Lipid Droplet Staining**

Mouse liver and jejunum samples were cold-embedded in OCT medium and frozen at -20°C. Cryosections (8 to 10 µm) were fixed in methanol/acetone (1:1) for 5 min and washed with PBS. CD36 was immunolabeled exactly as described above. LDLR staining was performed using the rabbit anti-hLDLR (1:500) and Alexa Fluor 555-conjugated anti-rabbit IgG antibodies. For lipid droplets staining, sections were fixed in 4% paraformaldehyde for 5 min, washed with PBS and incubated for 45 min at 20°C with 1 µg/ml of the fluorescent neutral lipid stain Bodipy 493/503 (Life Technologies). After washing, sections were counterstained with DAPI and mounted in Vectashield (Vector Laboratories). Formalin-fixed, paraffin-embedded perigonadal adipose tissue samples were cut into 5-µm-thick sections, deparaffinized and submitted to antigen retrieval by heating at 100°C in 10 mM citrate buffer pH 6.0 for 20 min. Sections were blocked and incubated as above using the anti-mCD36 (1:500) and Alexa Fluor 488-labeled anti-goat secondary antibody. Immunolabeled tissue sections were analyzed by confocal microscopy.

**Quantitative Real-Time PCR**

Total RNA was isolated from tissue samples using RiboZol (Amresco) and used as templates for cDNA synthesis using qScript cDNA SuperMix according the manufacturer's instructions (Quanta Biosciences). Quantitative real-time PCR (qPCR) was performed with the Mx3000P

real-time thermal cycler (Agilent) using the PerfeCTa SYBR Green SuperMix, UNG, Low ROX (Quanta Biosciences) and specific forward and reverse oligonucleotide primers (listed in Table S1). Dissociation curves and agarose gel electrophoresis were performed to verify that a single product was amplified. At least three independent experiments were done in duplicates. The cycle threshold (Ct) value of each gene was normalized against that of the housekeeping gene hypoxanthine guanine phosphoribosyl transferase (HPRT) and the relative level of expression calculated using the comparative ($2^{-\Delta\Delta CT}$) method.

**Statistical Analysis**

All experiments were performed at least three times and representative results are shown in figures. All data are presented as means ± SEM. Statistical significance was determined using the Student's *t*-test. A *P* value of $< 0.05$ was considered significant.

**Supplemental References**


1. Poirier S, Samami S, Mamarbachi M, Demers A, Chang TY, Vance DE, Hatch GM, Mayer G. The epigenetic drug 5-azacytidine interferes with cholesterol and lipid metabolism. *J Biol Chem*. 2014;289:18736-18751
2. Luiken JJ, Dyck DJ, Han XX, Tandon NN, Arumugam Y, Glatz JF, Bonen A. Insulin induces the translocation of the fatty acid transporter fat/CD36 to the plasma membrane. *Am J Physiol Endocrinol Metab*. 2002;282:E491-495

# Supplemental Figures

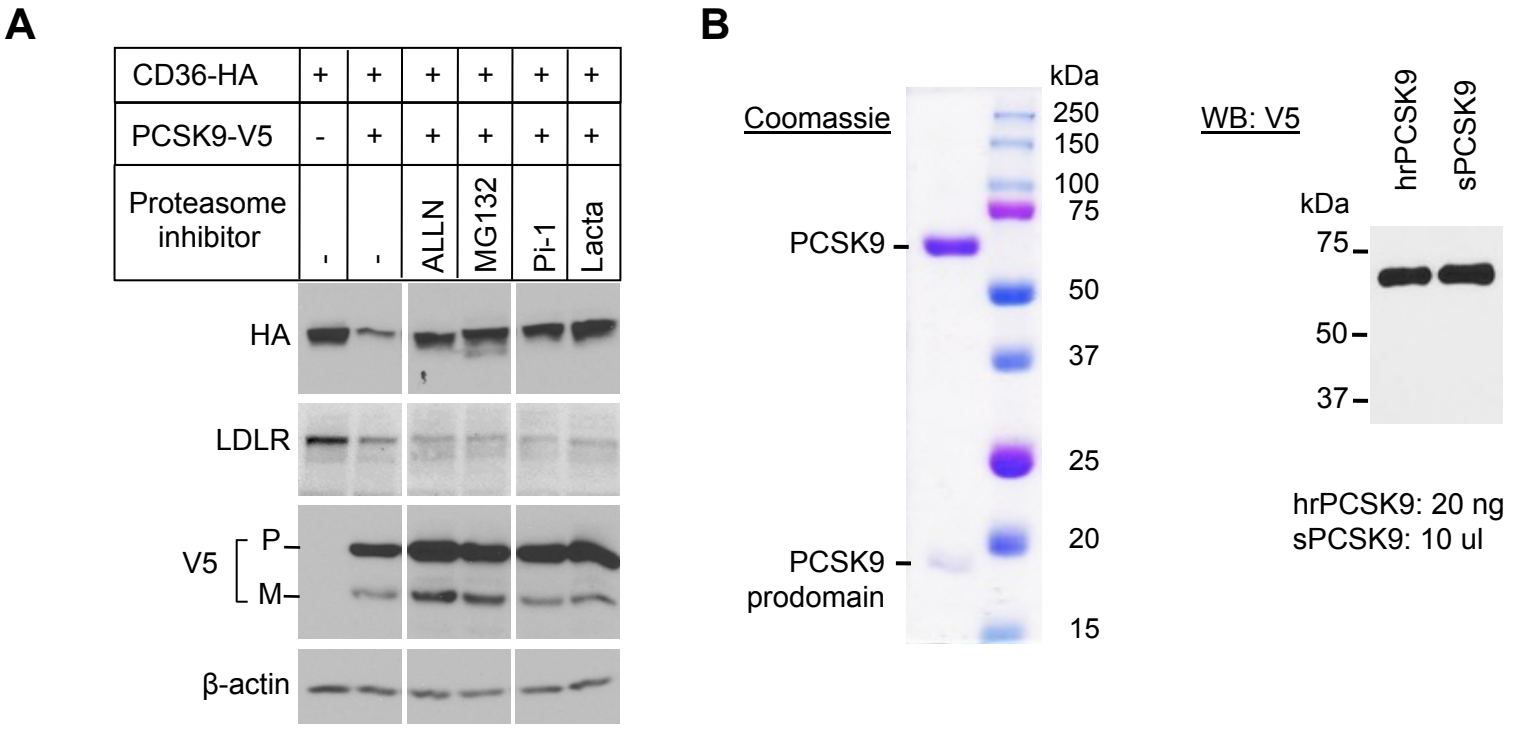


**Supplemental Figure I.** (**A**) Proteasomal inhibition of PCSK9-mediated CD36 degradation. HEK293 cells transfected with CD36-HA and either an empty pIRES-V5 vector (-) or PCSK9-V5 were incubated with proteasome inhibitors ALLN (20 μM), MG132 (2.5 μM), proteasome inhibitor-1 (PI-1; 5 μM) or lactacystin (20 μM) for 16 h. Cell lysates were subjected to Western blotting with the anti-HA, anti-hLDLR, anti-V5-HRP and anti-β-actin antibodies. Theses data are representative of at least three independent experiments. (**B**) Coomassie staining of purified recombinant hPCSK9 (1.4 μg) resulting from the last purification step by size exclusion chromatography showing the mature form and prodomain of PCSK9 (left panel) and WB (anti-V5) of purified rhPCSK9 (20 ng) and conditioned media (10 μl) from HEK293 cells overexpressing PCSK9-V5 (sPCSK9) (right panel).

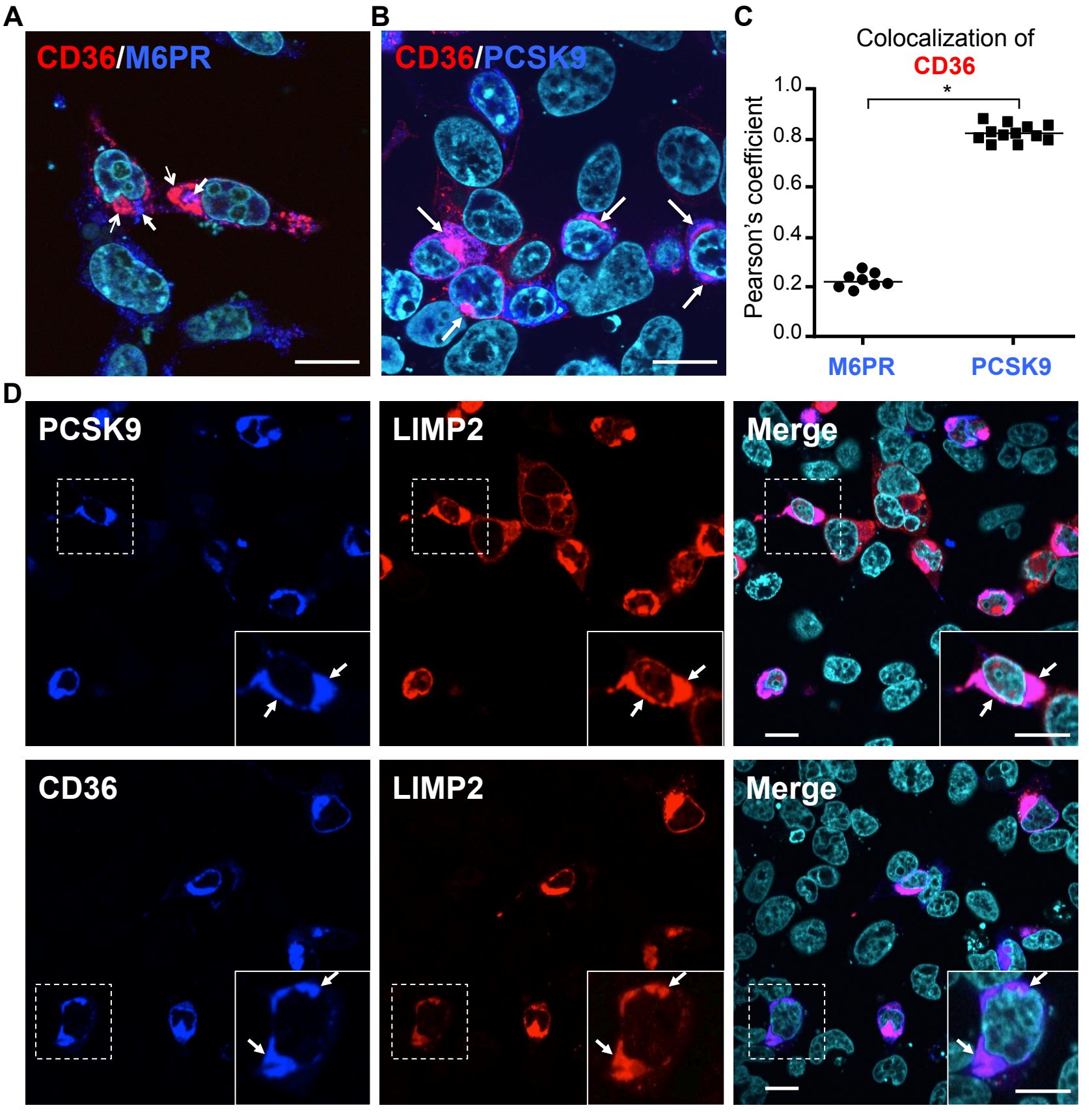


**Supplemental figure II.** CD36 colocalizes with PCSK9 in lysosomes. (**A, B, D**) Immunofluorescence of HEK293 cells transfected with pIRES-CD36-HA and pIRES-PCSK9-V5 (A, B) or triple-transfected with pIRES-PCSK9, pIRES-CD36-V5 and pIRES-LIMP2-HA (D) in the presence of 2.5 μM MG132. Immunolabeling was performed under permeabilizing condition with the anti-M6PR (blue) and anti-HA (red) (A), anti-V5 (blue) and anti-HA (red) (B), anti-hPCSK9 (blue) and anti-HA (red) (D) (upper panels), or anti-V5 (blue) and anti-HA (red) (D) (lower panels). Nuclei were stained using DAPI (cyan). Closed arrows (M6PR) and open arrows (CD36) indicate low levels of colocalization (A) and contrast with colocalization of CD36 and PCSK9 (B; arrows, purple color). (**C**) Degree of colocalization (Pearson's correlation coefficient (r) value) between CD36 and M6PR and between CD36 and PCSK9, *, *P*<0.01, mean ± s.e.m. (**D**) Colocalization (arrows, inset) of PCSK9 with LIMP2 or CD36 with LIMP2 is exemplified by the purple color in the merge images. Bars, 20 μm. Images are representative of n=3 independent experiments.

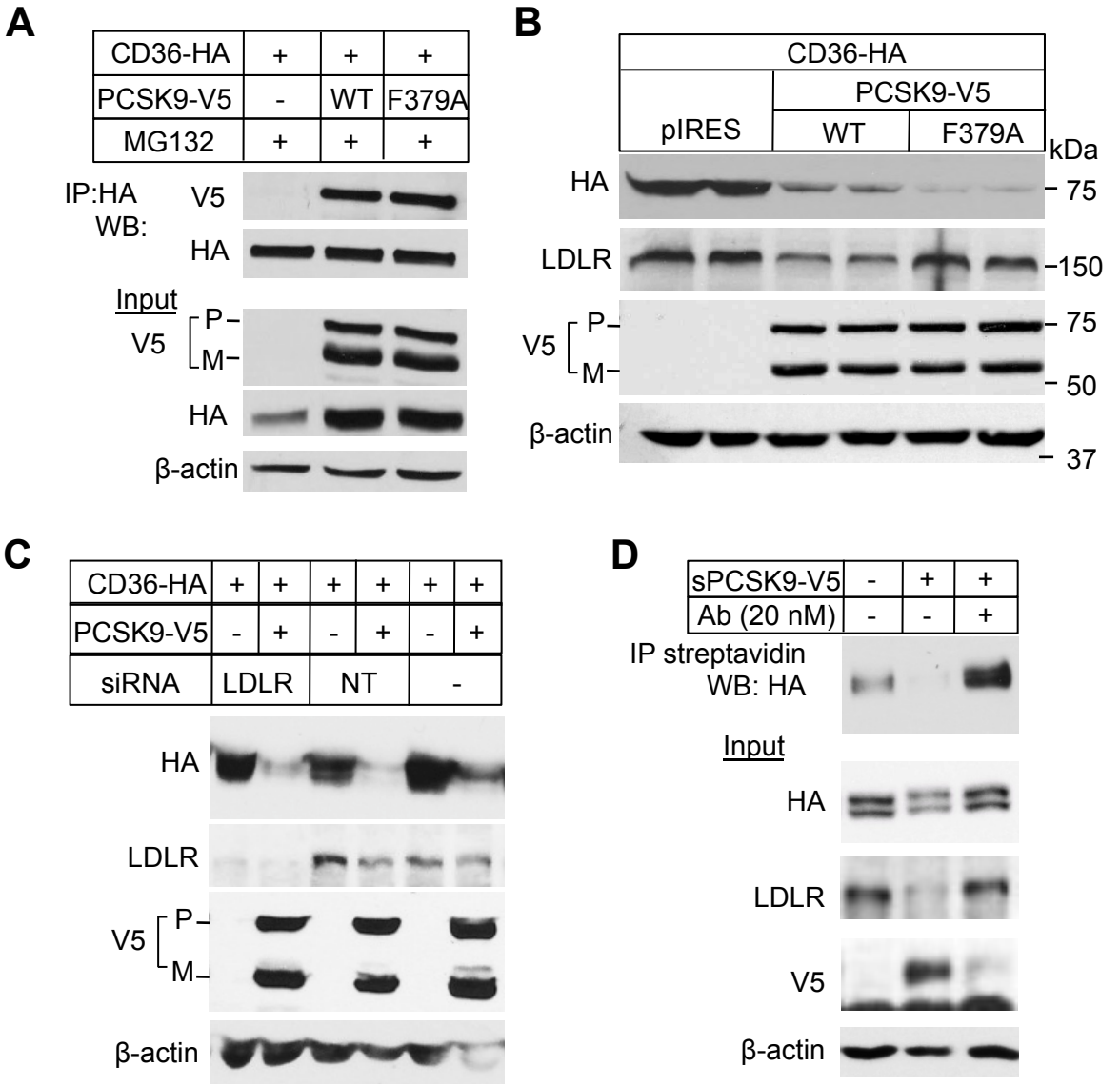


**Supplemental Figure III.** (**A**) CoIP of WT PCSK9 or the F379A mutant with CD36 in HEK293 cells transfected with CD36-HA and either pIRES-V5 (-), PCSK9-V5 (WT) or the PCSK9-F379A-V5 mutant in presence of MG132 (2.5 μM). Protein levels of CD36-HA, PCSK9-V5 and β-actin before IP (input) are shown. (**B**) PCSK9-F379A induces the degradation of CD36 but not of LDLR. HEK293 cells were transfected as described in (A) in the absence of MG132. Forty-eight hours post-transfection, total CD36-HA, LDLR, PCSK9-V5 and β-actin protein levels were analyzed by Western blotting. (**C**) PCSK9-mediated CD36 degradation is LDLR-independent. HEK293 cells were transfected either with a non-targeting siRNA (NT) or a siRNA targeting LDLR or left untransfected (-) and 48 h later, cells were co-transfected with CD36-HA and either with pIRES-V5 or PCSK9-V5 for 24 h before WB analysis as described in (B). (**D**) A PCSK9 neutralizing antibody inhibits PCSK9-induced CD36 degradation. Stable HepG2-CD36 cells were incubated with serum-free medium (-) or with conditioned media of HEK293 cells overexpressing PCSK9-V5 (sPCSK9) in the absence or presence of a PCSK9 blocking antibody (Ab; 20 nM). After 16 h, cell-surface proteins were biotinylated and cell lysates were incubated with streptavidin-agarose and analyzed by WB for CD36 (anti-HA). Protein levels of CD36-HA, LDLR, PCSK9-V5 and β-actin before affinity-precipitation (input) are shown. Theses data are representative of at least three independent experiments.

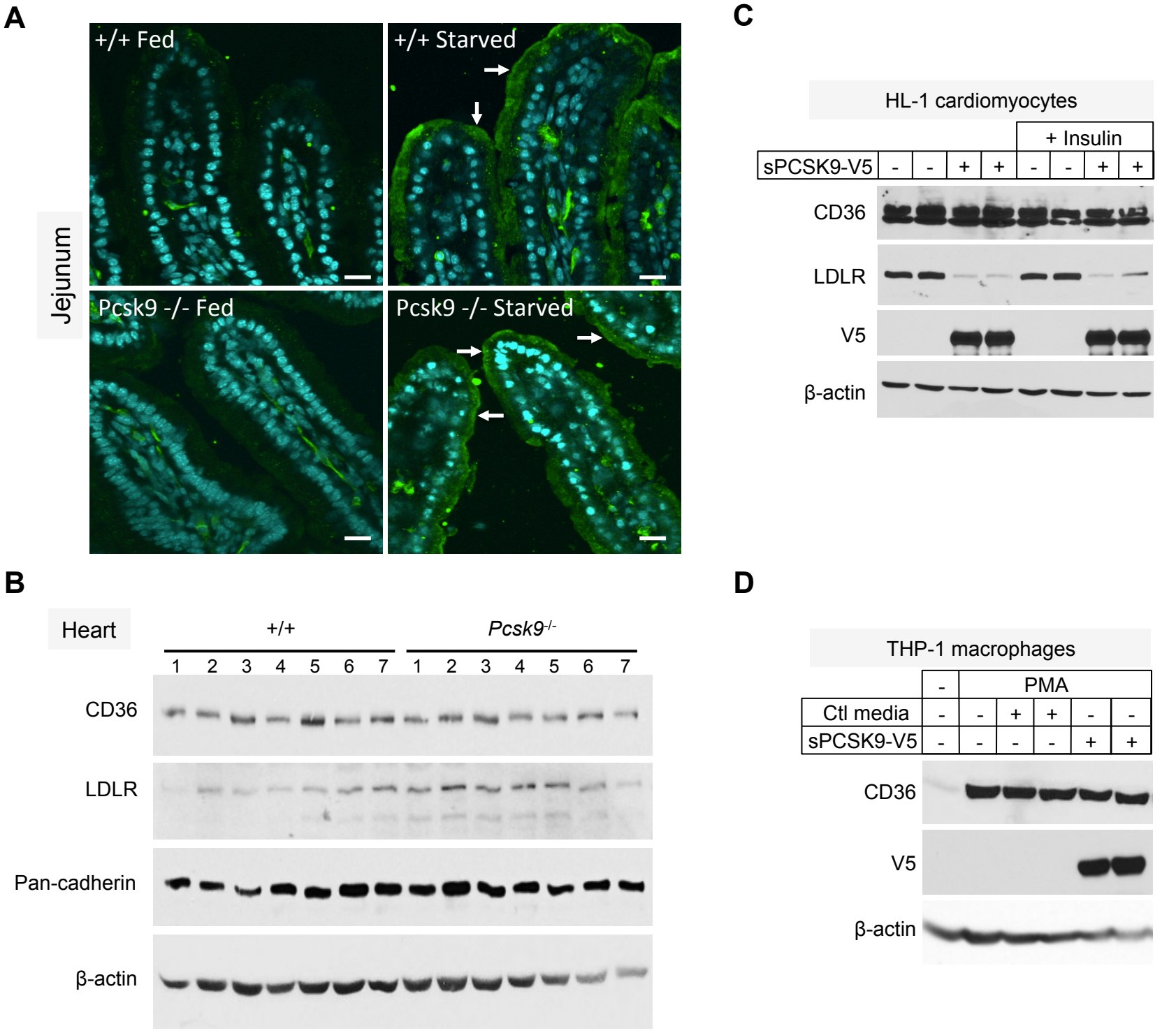


**Supplemental Figure IV.** Cell and tissue-type dependent degradation of CD36 by PCSK9. (**A**) Immunofluorescence of CD36 in the jejunum of C57BL/6 (+/+) and *Pcsk9*$^{-/-}$ mice under fed and starved conditions. Arrows show the labeling of CD36 at the apical brush border membrane of villi. Images are representative of n=3 independent experiments. Bars, 20 um. (**B**) WB of CD36, LDLR, pan-cadherin and β-actin in mouse heart tissue lysates from +/+ and *Pcsk9*$^{-/-}$ mice. (+/+, n=7 mice; *Pcsk9*$^{-/-}$, n=7 mice). (**C-D**) HL-1 cardiomyocytes treated with or without 167 nM insulin to induce membrane translocation of CD36 (**C**) or PMA-differentiated THP-1 macrophages (**D**) were incubated for 16 h with conditioned media obtained from HEK293 cells overexpressing V5-tagged PCSK9 (sPCSK9) or control media (Ctl media, DMEM (-) and pIRES-V5 (+)). Cell lysates were subjected to WB for mouse CD36, mouse LDLR, PCSK9-V5 and β-actin (C) or human CD36, PCSK9-V5 and β-actin (D).

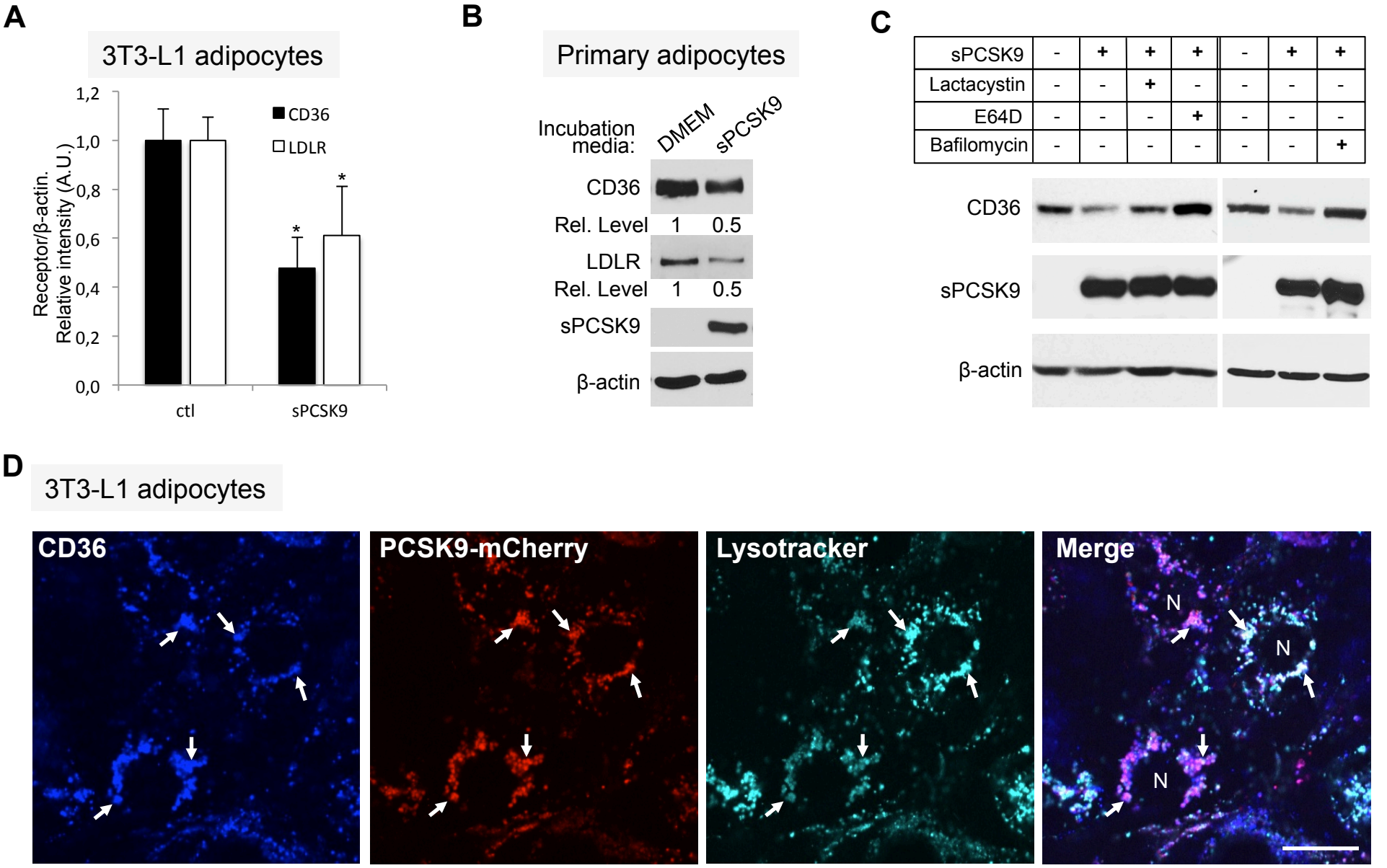


**Supplemental Figure V. (A)** Quantification of CD36 and LDLR protein band intensity (normalized over β-actin) after WB from differentiated 3T3-L1 adipocytes incubated with sPCSK9 for 16 h. *, *P*<0.01 *versus* control. n = 3 independent experiments performed in triplicates. (**B**) WB of primary adipocytes isolated from mouse perigonadal adipose tissue and incubated with sPCSK9 for 16 h. Quantification of CD36 and LDLR protein band intensities were normalized over β-actin. These data are representative of at least three independent experiments. (**C**) WB of differentiated 3T3-L1 adipocytes incubated with sPCSK9 in the absence or presence of the proteasome inhibitor lactacystin (20 μM), the lysosomal cysteine proteases inhibitor E64D (10 uM) or the lysosome vacuolar type H+-ATPase (V-ATPase) inhibitor bafilomycin A1 (100 nM) for 16 h. (**D**) Colocalization of CD36 and PCSK9 in lysosomes of 3T3-L1 adipocytes. 3T3-L1 adipocytes were incubated for 16 h with PCSK9-mCherry and the goat anti-mCD36/anti-goat Alexa-647 antibodies in the presence of 2.5 μM MG-132 prior addition of 500 nM LysoTracker® Blue DND-22 for 2 h. Representative confocal immunofluorescence images show extensive colocalization (arrows) of CD36, PCSK9 and Lysotracker. N, nucleus. Omission of the primary goat anti-mCD36 antibody was used as a negative control and showed no specific staining (not shown). Bar 20 μm.

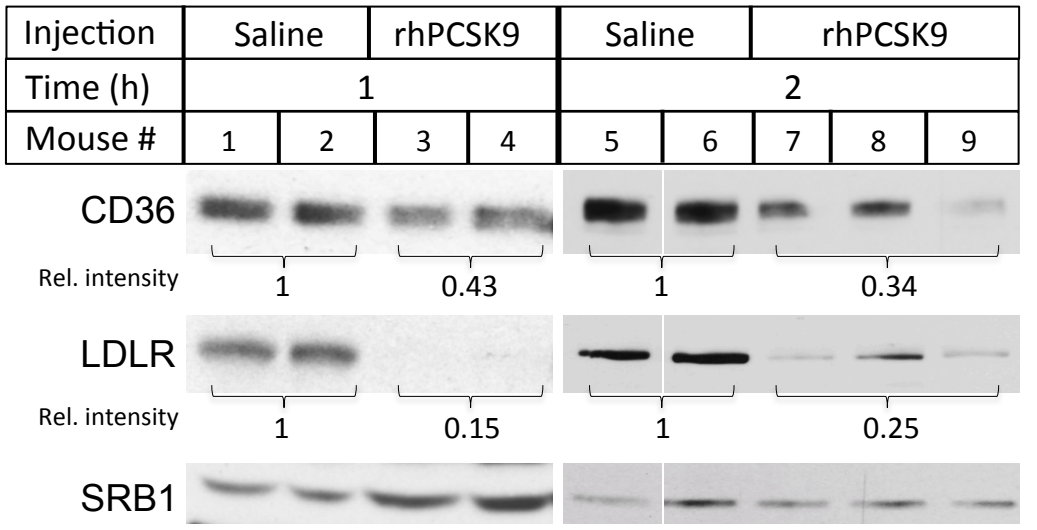


**Supplemental Figure VI.** Reduction of hepatic CD36 protein levels in mice injected with recombinant PCSK9. Wild-type C57Bl/6 mice were tail-vein injected with 0.9% NaCl (saline) or 32 µg rhPCSK9 and the liver was removed 1 h (n = 2 mice/condition) or 2 h (n = 2 mice for saline and n = 3 mice for rhPCSK9) after injection for Western blotting analysis with antibodies against mouse CD36, LDLR and SR-B1. Mean relative intensities of CD36 and LDLR were normalized to SR-B1 using the NIH ImageJ software.

# Supplemental Table

## Table SI

Oligonucleotides used for quantitative PCR

| Gene | Primer Sequences (5' → 3') |
|---|---|
| Mouse CD36 | Forward GATGACGTGGCAAAGAACAG<br>Reverse TCCTCGGGGTCCTGAGTTAT |
| Mouse LDLR | Forward GGAGATGCACTTGCCATCCT<br>Reverse AGGCTGTCCCCCCAAGAC |
| Mouse HPRT | Forward CAGCGTCGTGATTAGCGATG<br>Reverse CAGAGGGCCACAATGTGATGG |